Recent developments in the use of electrokinetic methods for rapid cell viability assessments and separations

Blanca H. Lapizco-Encinas[†,*]

[†] Microscale Bioseparations Laboratory and Biomedical Engineering Department, Rochester Institute of Technology, 160 Lomb Memorial Drive, Rochester, New York, 14623, United States.

*Email: bhlbme@rit.edu

Abstract

Rapid cell viability assessments are essential in a growing number of fields, including clinical analysis, healthcare, drug development and food safety. Electrokinetic (EK) methodologies have proved to be robust and reliable platforms of the analysis of cells, including viability assessments. Discussed here are applications of two EK phenomena, dielectrophoresis and electrophoresis, which can discriminate cells by their viability status and also sort and separate cells into separate viable and nonviable fractions, so further analysis can be performed. For each EK method, the operating principle is presented, followed by a brief historical overview and a detailed analysis of recent reports published between 2015-2024. The concluding remarks include a summary of the content of this review article and present a future perspective on the expected future advances on EK-based systems for the assessment and separation of cells based on their viability status.

Keywords:

Cells

Dielectrophoresis

Electrokinetics

Electrophoresis

Viability

1. Introduction

The assessment of cell viability is essential in a growing number of applications and fields. Methods for the effective control and prevention of infections are urgently needed due to the increasing number of deaths and infections worldwide. In 2019 the Centers for Disease Control and Prevention of the U.S. reported a healthcare cost over 25 billion dollars associated with infectious diseases [1,2]. The advent of antibiotic resistant bacteria, for example, poses a major threat to the control and treatment of infectious diseases. The rapid assessment on the effect of antibiotics and other drugs on pathogenic bacteria, to identify the presence of antibiotic resistant strains has become vital in clinical and healthcare settings [3]. The field of medicine also requires effective methods for the rapid assessment of cell viability for testing the efficacy of new drugs, in particular anticancer drugs. Similarly, the development of new antibiotics requires significant testing of the effects of antibiotics on target pathogenic bacteria.

Besides clinical and healthcare applications, cell viability assessments are also an immediate need in the food industry, as early stage detection of pathogens in food matrices is a major challenge in food safety [4]. The incidence of food borne diseases has been increasing over the years, and early detection is key for minimizing the impact on human health [5]. An additional demand in the food industry is the assessment and quality control of food items that contain active microorganisms, such as probiotic and fermented products, functional foods, and dairy products. An effective technology that can enable rapid quantification of viable microorganisms present in these food items and food supplements would be a major asset. Another important example of the

immediate need of rapid cell viability approaches is the pharmaceutical industry, where continuous monitoring of the stress and viability of cell cultures is crucial [6]. Others fields, such as environmental monitoring, in particular in the treatment of wastewaters, also require effective methods for the monitoring of cell viability [7].

Electrokinetic (EK) phenomena, which can be used to manipulate fluids and particles employing electric fields, offer attractive characteristics for the analysis of microorganisms, as they depend on the dielectric properties of the cells, circumventing the use of chemical labels [8]. The combination of microfluidics and EK effects is highly relevant, as it can enable portable devices with short processing times, which can be ideal for on-line monitoring systems and remote sensing applications.

The present review article discusses two EK methods for rapid cell viability assessment and separation. The two EK phenomena that were selected for this discussion are dielectrophoresis (DEP) and electrophoresis (EP). The basis for this selection was that both methodologies are able to discriminate cells by their viability status and also sort and separate cells into viable and nonviable fractions, so further analysis can be performed. This review article aims to provide the reader with an overview of EK-based devices and technologies that can handle both operations simultaneously: viability assessment and separation. The technique of electrorotation (EROT) [9], while extremely powerful for viability assessments, cannot be used for continuous sorting and separation purposes, thus, it is not discussed in this article. Both, DEP and EP, are powerful analytical and separation techniques that do not require the use of labels, and can distinguish between live and dead cells by probing the dielectric properties of the cells. While DEP exploits differences in electrical polarization, EP exploits differences in electromigration velocity. The former is usually employed with high frequency AC electric fields, while the latter requires the use of DC or DC-biased low frequency AC electric fields. Although DEP has been successfully utilized to test the viability status of a wider variety of cell types (bacterial, yeast, mammalian and cancer cells), EP also has great potential, as its nonlinear mode offers additional capabilities on how EP can discriminate between live and dead cells [10,11]. This review article is organized as follows: The Introduction, which is Section 1, describes the importance of cell viability assessments and separations in a growing number of applications. Section 2 is focused on DEP-based studies on cell viability. First, the operating principle and fundamental equations are presented, followed by a brief historical overview and a detailed discussion on recent (2015-2024) studies. The majority of the reports discussed in this section demonstrated both processes, viability assessment and live/dead cell sorting/separation. Analogously, the third section describes the operating principle and fundamental equations of the EP-based studies, followed by brief description of the first EP-based viability cell separations and detailed discussion of relevant (2015-2024) studies. It is important to mention that all DEP-based reports employed microfluidic systems, while EP studies employed bench scale capillary electrophoresis (CE) systems and microfluidic systems. Section 4, includes the concluding remarks that summarize the content of this review article and present a perspective on the expected future advances on EK-based systems for the assessment and separation of cells based on their viability status.

2. Dielectrophoresis-based cell viability assessments and separations

Dielectrophoresis probes the dielectric characteristics of microorganisms and thus is an effective methodology for rapid viability separations and assessments, as dielectric properties are altered as a result in changes in viability status [12]. Dielectrophoresis is attractive as a viability assessment tool since it offers rapid response times, the potential for miniaturization and does not need labels or tags. Numerous reports have focused on the manipulation, sorting, separation and quantification of cells employing DEP, where careful consideration is given to preserve cell viability during DEP-based analysis [10,13–20]. Described below are the operating principle and applications of DEP designed specifically to distinguish and separate live from dead cells.

2.1 Dielectrophoresis operating principle

Dielectrophoresis is defined as the migration of particles due to polarization effects under the presence of a nonuniform electric field. Changes in dielectrophoretic migration reflect alterations in the cell's polarizability with respect to that of the suspending medium. When a cell dies, its dielectric properties are altered, which in turn alters the dielectrophoretic response of the cell. The dielectrophoretic force ($\mathbf{F}_{DEP}$) and velocity ($\mathbf{v}_{DEP}$)_exerted on a spherical cell are defined as follows:

$$\mathbf{F}_{DEP} = 2\pi r_p^3 \varepsilon_m \mathrm{Re}[f_{CM}] \nabla E^2, \text{ where } f_{CM} = \frac{\varepsilon_p^* - \varepsilon_m^*}{\varepsilon_p^* + 2\varepsilon_m^*} \quad (1)$$

$$\mathbf{v}_{DEP} = \mu_{DEP} \nabla E^2, \text{ where } \mu_{DEP} = \frac{r_p^2 \varepsilon_m}{3\eta} \mathrm{Re}[f_{CM}] \quad (2)$$

where r_p refers to the cell radius, the magnitude of the electric field is represented by E, and Re[f_{CM}] is the real part of the Clausius-Mossotti factor, which accounts for the polarizability of the particle/cell compared to that of the suspending medium. The parameter f_{CM} depends on the complex permittivity of the particle/cell and the suspending medium and the frequency of the electric field, and it varies from -0.5 to 1.0 for spherical cells [21]. The complex permittivity ε^*, in turn, depends on the real permittivity (ε) and the real conductivity (σ) of the particle/cell ($\varepsilon_p^* = \varepsilon_p - (j\sigma_p/\omega)$) and the medium ($\varepsilon_m^* = \varepsilon_m - (j\sigma_m/\omega)$), respectively. The parameter ω is the angular frequency of the electric field and the parameter j is defined as $j = \sqrt{-1}$. In the expression for $\mathbf{v}_{DEP}$ μ_{DEP} is the dielectrophoretic mobility and η is the suspending medium viscosity. The sign of the parameter Re[f_{CM}] dictates the direction of the DEP force exerted on a cell, positive DEP (pDEP), obtained at positive values of Re[f_{CM}], is when cells migrate towards the regions of higher field gradient, while negative DEP (nDEP) is when cells are repelled from these regions. By looking at **Eqn. (1),** it is possible to discern that the characteristics of a cell that can vary as a result of viability loss are the dielectric properties (ε_p and σ_p) and cell size (r_p). Variations in ε_p and σ_p are directly reflected in the values of the Re[f_{CM}]. Further, the value of Re[f_{CM}] also depends on the frequency ω, at lower values of ω the value of Re[f_{CM}] depends on the characteristics (ε_p and

σ_p) of the cell membrane while at high values of ω the Re[f_{CM}] is dictated by the characteristics (ε_p and σ_p) of the cell cytoplasm. Loss of viability modify the values of the ε_p, σ_p and ε_p^* of a cell, which in turn modify the value of Re[f_{CM}] as seen in **Fig. 1** for yeast and Human Embryonic Kidney (HEK) 293 cells, where a similar behavior is observed for eukaryotic and mammalian cells. In general, over a large frequency range (low to mid-range values) the DEP response of viable cells is nDEP while dead cells exhibit a pDEP response, this observation holds true for a wide range of operating conditions and cell types. The distinct cell responses illustrated in **Fig. 1** agree with the fact that the cell membrane properties determine the cell DEP response at lower frequency values. Cell membranes have an insulative nature, i.e., they possess a low conductivity; however, when a cell dies, the cell membrane becomes compromised and it gets contaminated with the highly conductive cytoplasm, resulting in a significant increase of the cell membrane conductivity and polarizability. This explains why from low to mid-range frequency values dead cells exhibit pDEP while live cells with their nonconducting membranes exhibit nDEP behavior. In contrast, at high frequencies, live cells will usually exhibit pDEP and dead cells could exhibit nDEP or negligible DEP (**Fig. 1A**). This distinct behavior of dead cells from that of live cells can be used to effectively separate and discern live from dead cells [22].

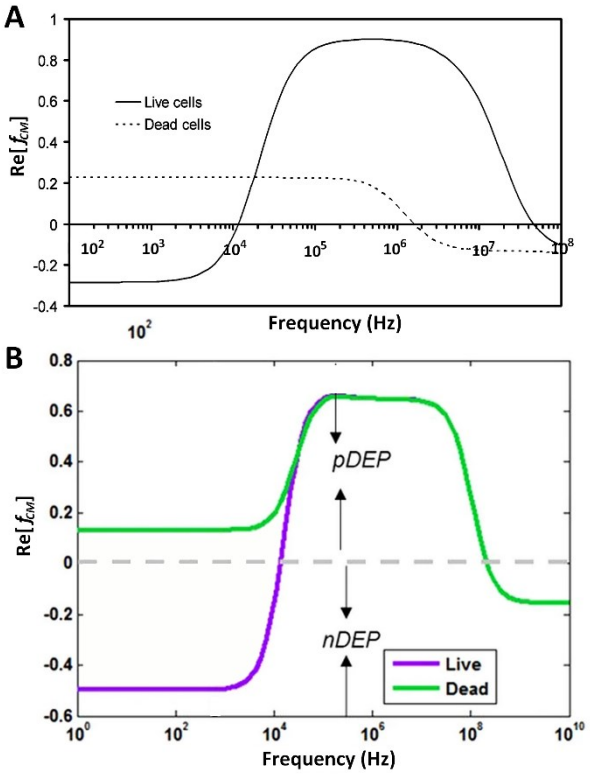

Fig. 1. Values of the real part of the Clausius-Mossotti factor as a function of the frequency of the electric field for live and dead cells. **(A)** Yeast cells, theoretical values estimated by Patel and Markx employing the multishell model. Adapted with permission from [22], copyright (2008) Elsevier. **(B)** HEK-293 cells, theoretical values estimated by Punjiya et al. employing the double-shell model. Adapted from [19], open access article distributed under a Creative Commons Attribution (CC BY) License, copyright (2021) Punjiya et al. In both plots, over a large frequency range, the dead cells exhibit positive values of the real part of the Clausius-Mossotti factor while live cells exhibit negative values, confirming that cell dielectric properties are affected by viability losses.

2.2 Reports on dielectrophoretic-based cell viability assessments and separations

The potential of DEP as an effective technique for discriminating between live and dead cells was unveiled 15 years after the first report on DEP in 1951 by Herbert Pohl [23]. The separation between live and dead yeast cells was reported by Pohl and collaborators in 1966 and 1968 [24,25]. In these experiments carried out at high frequencies (2.55 MHz), live cells exhibited pDEP behavior and were attracted towards a pin electrode and collected, which is in agreement with **Fig. 1A**. Dead cells, on the other hand, did not exhibit an observable response and remained in the suspending medium, unaffected. Also in agreement with **Fig. 1A** is the observation of dead yeast cells collecting at the electrode at low frequencies under pDEP effects and then repelled under nDEP effect when the frequency was increased to 2.55 MHz [25], as the response for dead cells varies from positive to negative as frequency increases. A summary of all the reports reviewed in this section is included in **Table 1**.

2.2.1 Bacteria cells

Recent reports on the use of DEP for viability assessments have demonstrated novel approaches and the applicability of DEP across diverse cell types. Bacterial viability assessments are of particular interest in clinical applications to detect pathogenic infections and for the testing of antimicrobial/antibiotic reagents. As mentioned, significant effort has been devoted to ensuring the DEP treatment of cells does not affect cell viability, ensuring that cells can be used/studied after DEP analysis [10,13–20] and to determine the effect of DEP on cell viability [7,14,26]. Sorting between live and dead bacterial cells is one of the most important applications of DEP.

The Agah group developed a unique approach that employed 3-dimensional insulator-based DEP devices that effectively trapped bacterial cells (*E. coli*) at low applied voltages using DC-biased AC voltages [27]. Employing this novel design, the Agah group reported the effective sorting between live and dead *Staphylococcus aureus (S. aureus)* and *Staphylococcus epidermidis (S. epidermis)* cells [28–30]. This group developed unique device designs that combined the benefits of electrode-based DEP and insulator-based DEP systems by employing devices with 3D embedded insulating micropillars, where the pillars compressed the flow also along the channel width and height. The presence of the pillars generated the necessary electric field gradients for DEP effects to occur. Employing AC potentials applied through passivated electrodes, they were able to selectively trap live *S. aureus* cells while dead cells kept flowing as shown in **Fig. 2A** [28]. In follow-up studies, they employed DC-biased AC fields to achieve the distinction between live and dead *S. aureus* cells [29] and live and dead *S. epidermidis* cells [30]. The latter report employed off-chip electrodes for stimulating the system and used impedance spectroscopy to assess cell viability. A recent study by the Tegenfeldt group [8] combined DEP and deterministic lateral displacement (DLD) to develop the method of EK-DLD for the

effective sorting between live and dead *E. coli* and *Saccharomyces cerevisiae* (*S. cerevisiae*) cells employing AC potentials. Their proposed technique is a powerful approach, as DEP exploits differences in EK properties while DLD exploits differences in size. This was a follow up study on their charge-based separation technique [31]. In this cell focused work [8] they performed a continuous charge-based cell sorting between live and dead *E. coli* cells, the employed device and their results are shown in **Fig. 2B**. The sorting device has three distinct outlets that allowed for collection of separated cell fractions. The sorting process was successful, as the sample that contained equal proportions of live and dead cells, was separated as follows: 72% of the live *E. coli* cells were collected at the displacing reservoir, with a 90% purity. Similarly, 63% of the dead cells were collected at the zigzag reservoir, with a purity above 90%. The intermediate reservoir contained a mixed fraction. The separation took 90 minutes, and the authors discussed that a difference in zeta potentials of 8 mV between the live and dead *E. coli* cells is the parameter that made the separation process. A major finding from this study was the fact that for *E. coli* cells a significant change in the cell zeta potential (ζ_P) was observed as a result of the heat-based cell inactivation process; live cells had a zeta potential of -42 mV, while a value of -34 mV was reported for dead cells (measured with a Zetasizer™). This is a net difference of ~8 mV, which is more than enough for efficient charge-based separation as demonstrated in recent reports [31,32]. However, this was not the case for live and dead for *S. cerevisiae* cells, were both cell populations, live and dead, had a cell zeta potential ~ -19 mV, that is, there was no discernible change in cell zeta potential as a result of the heat-based cell inactivation process. Regarding changes in cell size, the authors mentioned that no significant change in size was observed for dead *E. coli* cells compared to live ones; however, dead *S. cerevisiae* cells were found smaller (3.80 ± 0.44 μm) than live ones (4.70 ± 0.63 μm) [8]. These are important observations, and the contrasting results may be due to the distinct cell types studies, as *E. coli* cells are prokaryotic bacteria and *S. cerevisiae* cells are eukaryotic unicellular fungi. Given that the differences between live and dead cells depend on cell type, the separation process must be adapted accordingly. For the live and dead *E. coli* cell separation, the parameter exploited was charge differences in terms of ζ_P (results in **Fig. 2B**). However, for the live and dead *S. cerevisiae* cell separation (performed at much higher frequency of 20 kHz), differences in cell size were represented by differences in the dielectrophoretic mobility (μ_{DEP}) of the cells (Eqn. 2). The separation took place by exploiting differences on μ_{DEP}, which depends on both, cell size and dielectric properties. The authors stated that two distinct separation mechanisms were observed in their study, a charge-based mechanism and a DEP-mobility-based mechanism, and that more studies are still needed [8].

Antibiotic efficacy testing is another major application of DEP-based viability assessments. The Swami group has studied extensively the bacterium *Clostridium difficile* (*C. difficile*) due to its prominence as one of the major causes of antibiotic-induced enteric infections with high disease recurrence after antibiotic treatment [33–35]. In particular, they reported the dielectrophoretic fingerprinting of *C. difficile* strains to distinguish between high toxicogenic and non-toxicogenic cells [33]; and the DEP-based assessment of the efficacy of employing

probiotic microorganisms as inhibitor of *C. difficile* growth and toxicity [34]. In a more recent report [35], this group studied the efficacy of vancomycin against *C. difficile* employing pDEP and confirmation with electrorotation (EROT). Current methodologies for assessing antibiotic susceptibility require time-consuming bacterial culture, which can take over 16 hours to produce a result when employing the antibiotic at its minimum inhibitory concentration (MIC). The Swami group identified that cell exposure to MIC levels of vancomycin decrease the cytoplasmic conductivity of *C. difficile*, a change that can be assessed with DEP at high frequencies (since under high frequencies the Re[f_{CM}] is determined by the properties of the cell cytoplasm). **Fig. 2C.i** depicts the employed device which featured triangular insulating structures that created a sharp constriction. High frequency electric fields were applied through the platinum electrodes shown in the image. By testing two distinct concentrations of vancomycin that were close to the MIC levels, it was found that a concentration of 2 mg/L was effective at inactivating/killing the *C. difficile* cells, as illustrated by their DEP response in **Fig. 2C.ii**. The results are illustrated by three panels, obtained with untreated cells, and cells treated with 1 and 2 mg/L of vancomycin, respectively. Untreated live cells exhibit only pDEP response, cells treated with 1 mg/L have a mixed response, exhibiting both pDEP and nDEP; while cells treated with 2 mg/L exhibit only nDEP, indicating a strong decrease in their cytoplasmic conductivity, i.e., cell death. Thus, a vancomycin level of 2 mg/L is necessary for complete inactivation of *C. difficile* cells, this result was achieved only after 4 hours of treating the cells with vancomycin. At the high frequency employed, the inactivated/dead *C. difficile* cells exhibit nDEP due to the decrease in their cytoplasmic conductivity compared to live cells which exhibit pDEP. This study demonstrates how the ability for DEP to discern between live and dead cells can be employed for the rapid and effective assessment of antibiotic efficacy. The Gupta group also employed rapid DEP assessments to determine the efficacy of antibiotics [36,37]. The former study focused on DEP-based viability assessment of *E. coli* and *Salmonella Typhi* (*S. Typhi*) cells and by detecting cell membrane rupture (cell death) as a result of cell exposure to sushi S3, an antimicrobial peptide [36]. In the latter report, the Gupta group developed the technique called DEPIS, a combination of DEP with impedance spectroscopy (IS), for the rapid assessment of cell viability and antimicrobial susceptibility [37]. They studied *S. Typhi*, *Enterococcus faecalis* (*E. faecalis*) and *S. aureus,* which were treated with several antimicrobial agents: polymyxin B sulfate, sushi S3 peptide, levofloxacin, bacitracin, and methicillin. Cells exposed to the antibiotic agents were then introduced into the DEPIS device, where they were enriched by DEP forces and screened by IS, the entire process took only 60 min. In contrast with their previous work [36], the antimicrobial agents in this study had distinct cellular targets (cell membrane, cell cytoplasm and cell wall), so each antimicrobial agent produced a distinct set of changes on the cells, justifying why impedance spectroscopy was used to rapidly assess cell viability. The authors concluded that ionic release from dying cells is an effective and rapid way to assess cell viability and antibiotic efficacy [37]. Further, they also demonstrated the rapid distinction between methicillin-resistant and methicillin-susceptible *S. aureus* strains, which can be critical in clinical settings.

Ensuring that all pathogens in a sample have been eliminated is another important application. Devices for cell inactivation were reported by the Yang group [38–40], they employed channels with insulating micropillars and chambers filled with silica microbeads to allow DEP forces to irreversibly electroporate *E. coli*, *E. faecalis* and *S. cerevisiae* cells and cause cell death. In these systems DEP was not used for performing the viability assessment of the cells, DEP was used induce cell dead and cell viability by assessed off-device by standard spread plate counting.

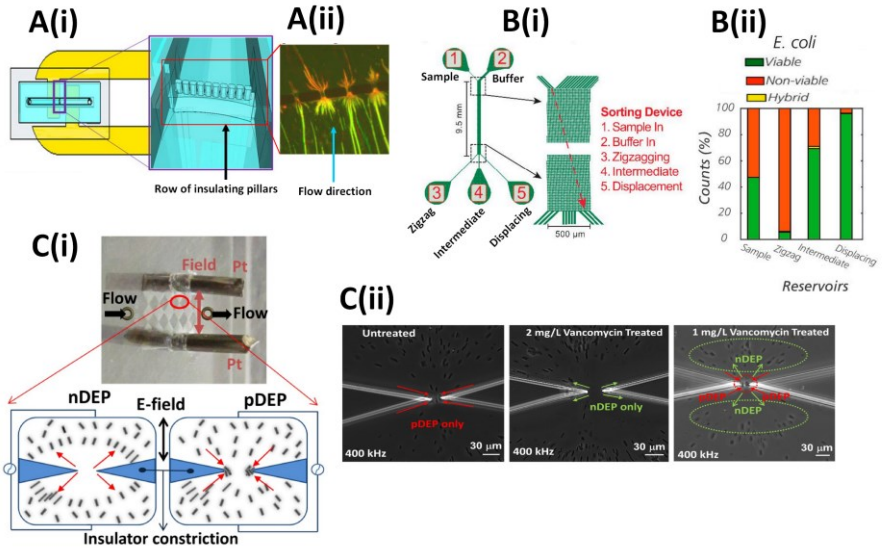

Fig. 2. Dielectrophoretic bacterial viability assessments. **(A.i)** Illustration of the device employed for the distinction between live and S. aureus cells, the device features a row of insulating pillars at the center of a microfluidic channel. **(A.ii)** Trapping of live S. aureus cells (dyed green) while dead cells (dyed red) are not trapped and continue flowing under an applied voltage of 400 Vpp at 30 kHz, flow direction is from bottom to top, and as observed in A.ii, mostly red cells are observed after the row of posts, green cells are not able to pass across the row of posts. Adapted with permission from [28], copyright (2015) AIP Publishing. **(B.i)** Illustration of the sorting device employed by Bo et al., the device features three outlet reservoirs, a sample reservoir and a buffer reservoir. The critical diameter of the device is 1.24 µm. **(B.ii)** Results from the sorting process illustrating effective discrimination between the live and dead *E. coli* cells. This sorting was obtained at 138 Vpp at 1 Hz, under a pressure of 20 mBar employing a medium with a conductivity of 100 mS/m. Adapted from [8], open access article distributed under a Creative Commons Attribution (CC BY) License, copyright (2020) Ho et al. **(C.i)** Illustration of the device employed by Rouhi et al. and two cartons to depict the cell response under nDEP and pDEP. **(C.ii)** DEP response of *C. difficile* cells left untreated and treated with 2 mg/L and 1 mg/L of vancomycin. A concentration of 2 mg/L is necessary for all cells to be indicated as demonstrated by their nDEP response. Adapted with permission from [35], copyright (2018) Elsevier.

2.2.2 Yeast cells

Dielectrophoresis-based viability assessments have also been developed for yeast cells. Discussed in **Section 2.2.1** is the study by Ho et al. [8], where they sorted live and dead *S. cerevisiae* cells by their DEP mobility at high frequency, as a charge-based sorting (as done for *E. coli*) was not possible. The Taguchi group [41] reported a unique study by developing devices for the discrimination between live and dead cells and also for cell fusion. They employed *S. cerevisiae* and red cabbage protoplast cells. Their device and discrimination process for live and dead *S. cerevisiae* cells are shown in **Fig. 3A**. They employed a microfluidic chamber with top and bottom thin electrodes, where live cells (non-stained) were attached to the electrodes by the effect of

pDEP, while dead cells (stained with methylene blue) were not attracted towards the electrodes and were flushed away employing fluid flow driven by syringe pumps. Their study also included live cell manipulation with pDEP and optical tweezers to achieve cell fusion with the addition of polyethylene glycol (PEG). The PEG was added to the cell suspension for two purposed, first, to make cells adhere to each other and second to trigger cell fusion [41]. In a follow up study [42], the Taguchi group analyzed the DEP response of live and dead yeast cells by inducing cell death on chip with bipolar electrodes by increasing the temperature (from 30 to 70 ºC) of the suspending media, cell death was observed above 50 ºC. They observed that live yeast cells exhibited pDEP and were attracted to the electrodes, but when the cells died, as a result of the increasing system temperature, the yeast cells moved away from the electrode. These observations are in perfect agreement with **Fig. 1A**, since at high frequency live cells exhibit pDEP while dead cells exhibit nDEP. This study demonstrates the flexibility of employing DEP for rapid and labeless cell viability assessments, as the cell response can be easily modified by modifying the frequency of the applied voltage. The García-Diego group [43] also demonstrated a rapid live/dead assessment for *S. cerevisiae* cells, they observed with microscopy that heat-killed yeast cells have broken down cell membranes. Further, they measured the DEP force exerted on live and dead cells employing a two electrode system where the electrodes were positioned forming a funnel configuration. Both cell types, live and dead, had exhibited pDEP behavior, but the DEP force decreased significantly on dead cells, i.e., dead cells still exhibited pDEP, but at a much lower magnitude than live cells. They explained these observations as the result of increased conductivity in the cell membrane and cell wall of the dead cells, since these two structures get contaminated with the cell cytoplasm. A continuous DEP-based sorter for live and dead yeast cells was reported by the Li research group [21]. They developed a unique design where DEP effects were enabled by two asymmetric orifices (one smaller, and one larger) located at the side walls of a microchannel as shown in **Fig. 3B.i**. Cells exhibiting pDEP (live cells) would migrate closer to the smaller orifice while cells exhibiting nDEP (dead cells) would migrate closer to the larger orifice as depicted in the cartoon and experimental results in **Fig. B.ii-B.iii**, respectively. The results are as expected under a high frequency of 10 MHz, where dead yeast cells have a negative response (**Fig. 1A**); they also observed that both cell types, live and dead, exhibited pDEP at a frequency of 1 kHz. In agreement with Ho et al. [8], dead cells were smaller in size than live ones. This novel design allowed for successful continuous sorting and separation processes, where the distinct cell fractions could be collected at distinct outlet reservoirs [21]. The Wenger group [44,45] also reported the separation between live and dead *S. cerevisiae* cells employing a complementary metal-oxide-semiconductor (CMOS) DEP-based device with interdigitated electrode arrays (IDEs). In their first study [44] they achieved the pDEP trapping of live and dead cells at a distinct frequency for each cell type, 3 MHz and 90 kHz for the live and dead cells, respectively, which is in perfect agreement with **Fig. 1A**. In their follow up study [45], the Wenger group demonstrated selective trapping of live yeast cells by means of pDEP while dead cells exhibited nDEP; they achieved a 100% collection of live cells at a frequency of 5 MHz with deionized water as suspending medium.

In agreement with previous studies, they reported that dead cells had an increased membrane conductivity, and a decreased cytoplasmic conductivity compared to live cells. The differences in conductivity values between live and dead cells were also exploited by Wu et al. [46] in a multiplexed system and by Bunthawin et al. [47] in a micro-parallel cylindrical electrodes system to separate live from dead yeast cells. All of these reports illustrate that effective distinction between viable and nonviable *S. cerevisiae* cells can be obtained with DEP by exploiting the differences in the cells' dielectric properties.

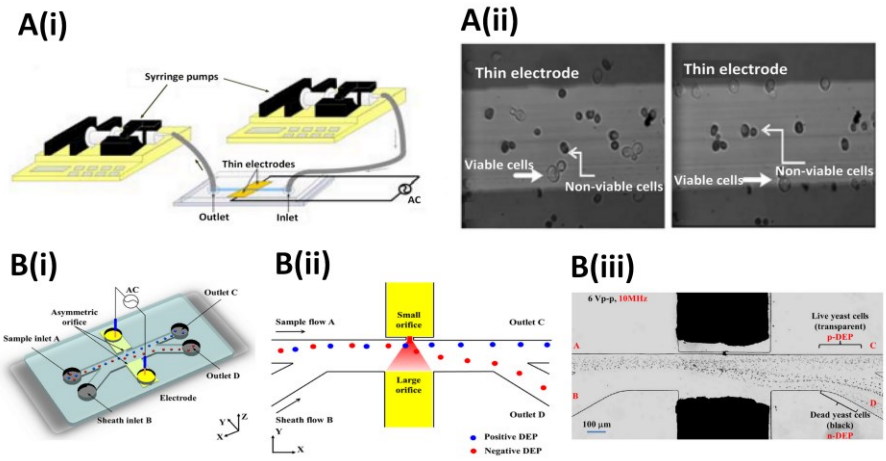

Fig. 3. Dielectrophoretic yeast cells viability assessments. **(A.i)** Illustration of the thin electrode device employed for distinguishing between live and dead *S. cerevisiae* cells. The device was connected to two syringe pumps. **(A.ii)** Image of the live (non-stained) and dead (stained with methylene blue) cells before and after the application of an AC voltage. Live cells are attracted to the electrodes under pDEP effects while dead cells show no response at a frequency between 300 kHz to 15 MHz. This frequency range was selected as it produce the distinct behavior of the live and dead cells. Adapted from [41], open access article distributed under a Creative Commons Attribution (CC BY-NC 4.0) License, copyright (2015) Mizuta et al. **(B.i)** Device with asymmetric orifices for DEP-based viability assessment. **(B.ii)** Cartoon depicting the expected migration of cells exhibiting pDEP and nDEP behavior. **(B.iii)** Experimental demonstration of the separation of live and dead *S. cerevisiae* cells suspended in deionized water where live cells exhibit pDEP and dead cells exhibit nDEP under 6 Vpp at 10 MHz. Adapted with permission from [21], copyright (2019) American Chemical Society.

2.2.3 Mammalian cells

Determination of cell stress due to nutrient depletion or harsh environmental conditions is essential in the production of biopharmaceuticals. Dielectrophoresis is a tool that can be used to assess the physiological state of mammalian cells, including the determination of cell apoptosis. The Bridges group [6,48–50] has studied extensively the changes in the dielectric properties of Chinese hamster ovary (CHO) cells as a result of starvation. In their more recent report [6] they employed a dual frequency DEP cytometry system to study the changes in the dielectric properties of CHO cells as a results of starvation-induced apoptosis. The dual frequency system assessed two specific properties, the membrane capacitance and the cytoplasm conductivity; the lower frequency (300 kHz) was tuned to probe the cell membrane while the higher frequency (6 MHz) was aimed to probe the cell cytoplasm. The conditions from this study differ from those in Sections 2.2.1 and 2.2.2, on bacteria and yeast cells; since in this case cells were not heat-killed, the CHO cells were starved and their transition from live cells to apoptotic cells occurred gradually. They observed that both the membrane

capacitance and cytoplasm conductivity decreased for apoptotic cells compared to viable ones, but the decline occurred in a different manner for each parameter during the progression of the apoptosis process. They carried out measurements over 64 hours and observed that cytoplasmic conductivity declined very slightly during the first 40 h, followed by a rapid decline; while membrane capacitance has a steady decline over the entire 64 h period. The authors stated that their device can be employed for monitoring the physiological state of cells in pharmaceutical process [6].

The viability of other types of mammalian cells has also been studied with DEP. The Flanagan group discriminated between live and dead neural stem and progenitor cells (NSPCs) in a study focused on enriching stem cells to determine their fate via DEP [51]. Their device, depicted in **Fig. 4A**, featured a large capacity electrode array that enabled the selective enrichment of viable NSPCs by means of pDEP from a sample containing live and dead cells, while nonviable cells were flushed away. Their objective was to process the cell sample at 7 Vpp at 1 MHz, until enough viable cells were trapped and enriched at the electrodes. Once enough cells were captured, the viable cells were then released by decreasing the frequency in 100 kHz increments and collected at distinct frequency bins from the outlet reservoir. A similar approach was performed with astrocyte progenitor cells in the same study [51]. This report illustrated that DEP is a valuable tool in the study of stem cells. The Martinez-Duarte group [52] also worked with stem cells by performing the separation between viable and nonviable rat adipose stem cells (RASCs) in a system featuring 3-dimensional carbon electrodes as shown in **Fig. 4B.i**. Their novel system was equipped with a robotic that "picked and transferred" target cells. Since live RASCs exhibited pDEP at a frequency of 100 kHz, while dead RASCs had a nDEP behavior, their separation was straightforward. The viability assessment of RASCs was one of the three distinct applications developed in this work, the two others being the separation between *Candida albicans* (*C. albicans*) from *Candida tropicalis* (*C. tropicalis*) cells and the separation of C. *tropicalis* from polystyrene beads. The Wood research group [53] studied the live/dead sorting of dental pulp stromal cells (DPSC) by combining surface acoustic waves (SAW) and DEP effects. Their unique system which utilized AC electric fields and lateral mechanical oscillations, successfully enriched live cells with pDEP, achieving separation efficiencies above 98%.The system was able to handle a high throughput of 10^4 cells/minute and operate in a continuous flow mode (majority of DEP system can handle throughput below 10^3 cells/min [54]). This system was also employed for the live/dead separation of *S. cerevisiae* cells [53]. This study provides an additional example of DEP, in this case enhanced with SAW, as an effective tool for discriminating between live and dead cells and separate them for further use or analysis.

The assessment of the physiological state of blood cells has also been reported with DEP-based systems. The Martinez-Duarte group [55] also reported the rapid discrimination between U937 live and dead monocytes employing a device with 3-dimensional carbon electrodes. After careful characterization of the DEP response of the monocytes, they identified that at a frequency of 300 kHz the dead monocytes exhibited nDEP while live monocytes were attracted to the edges of the electrodes by pDEP effects. In some cases, live monocytes trapped

in pearl-chain formations. **Fig. 4B** shows the trapped live monocytes and a plot of the results. Under a voltage of 20 Vpp at 300 kHz, 90% of the live monocytes were trapped while dead monocytes were flushed away employing a 1 μL/ min flow. The authors discussed that the use of low voltage increases cell viability and strengthens the potential for this type of assessment to be used for the enrichment of live monocytes in clinical applications. Viability analysis of human T-lymphocytes with DEP has been reported by the Nawarathna group [56] and the Lorenzo group [57]. The former study [56] was focused on enriching T-lymphocytes after the transfection step in CAR T-cell therapy, as only viable cells can be used in CAR T-cell therapy. They used Jurkat cells as proxies of the T-lymphocytes, since Jurkat cells have similar characteristics to T-lymphocytes. They developed a device with interdigitated electrodes that successfully separated a mixture of live and dead cells. Their system worked differently from other reports, since at 3 Vpp at 5 MHz they trapped dead cells with pDEP while and live cells, which exhibited a weaker pDEP effect than dead cells, were removed with fluid flow. The majority of the reports reviewed here use nDEP for dead cells and pDEP for live cells. Dead cells were obtained by means of electroporation, which may produce dead cells with distinct characteristics of those employed in other DEP-based viability assessments [56] . In the latter study, the Lorenzo group [57] also assessed the viability of T-lymphocytes, where dead cells were prepared by exposing the cells to seven freezing/thawing cycles. They developed a microfluidic device with castellated electrodes, a single inlet and two outlets, which allowed for the continuous sorting between live and dead T-lymphocytes. The electrodes were located on one side of the channel only, cells exhibiting pDEP would travel closer to the electrodes side and elute at the left outlet, while cells under nDEP would move away from the electrodes and elute at the right outlet. The separation was performed at a frequency of 1.5 x10^6 Hz, which allowed for the live/dead cell discrimination, as the cells responses were pDEP and nDEP for the live and dead T-lymphocytes cells, respectively. This study is another excellent example of the use of DEP for clinical assessments of blood cells. A study on the apoptosis of Jurkat cells was also reported by the Hughes group [59], this study is discussed in detail in the next section focused on cancer cells.

2.2.4 Cancer cells

The viability assessment of cancer cells is critical when evaluating the efficacy of cancer treatment or drugs and also for monitoring the progress of apoptosis processes. Thus, several DEP-based approaches have been developed to separate and sort viable and nonviable cancer cells. A particular characteristic of these systems is that the great majority comprise several inlet and outlet reservoirs that allow the collection of separate fractions. An example of this is the system developed by the He group [60] for the sorting between live and dead PC-3 human prostate cancer cells. Dead PC-3 cells were prepared by thermal treatment. They developed a device with liquid electrodes that featured a conductivity gradient to induce pDEP on target cells. The device featured four inlets and four outlets and allowed separating live from dead PC-3 cells in a continuous manner by exerting

strong pDEP on live cells and weak pDEP or nDEP on the dead cells at a frequency of 50 kHz. The results showed that almost 90% of the live cells were deflected to the target outlet which also contained 13.2% of dead cells, achieving a sufficient separation. This device also proved successful at separating human adipose-derived stem cells (ADSCs) from MDA-MB-231 cancer cells.

The Hughes group [59] developed a novel study focused on the quantification of apoptosis of HeLA cells. HeLA cells are of significant importance in the field of cancer research, HeLA are a cervical cancer cell line that allowed discerning how the human papilloma virus can cause cervical cancer. The study of the process of cell apoptosis is necessary for the development of new anti-cancer drugs. The Gascoyne group had reported in 2002 [61] that apoptosis could be detected by DEP, much earlier than with conventional methods, by detecting changes in the dielectric properties of the cell membrane. The Hughes group had explored the use of DEP to detect changes in cell dielectric properties, which they identify as changes in the cell phenotype, after treatment with anti-cancer drugs [62], and extended this methodology for assessing the series of stages in apoptotic progression [59]. They employed the commercially available system 3DEP (DEPtech), which has been used in several other cell studies [34,62–65]. The 3DEP system consists of a disposable well plate chip, the wells have electrodes on the side walls that enable DEP effects. Cell exhibiting pDEP are attracted to the well walls and trapped at the electrodes, while cells exhibiting nDEP are not trapped and flow through the center of the well, the farthest location from the well wall electrodes. To induce apoptosis the HeLA cells were incubated with staurosporine (1 μM suspension), a known apoptosis inducing agent. Then the HeLA cells were analyzed with the 3DEP device to obtain their DEP spectra, which consists of a plot of the relative DEP force (**Eqn. 1**) vs frequency. The DEP spectra was then fitted using the single shell model to obtain the dielectric properties of the cells and detect changes when comparing to the spectra of untreated cells. In particular, changes in the parameters of cytoplasmic conductivity and membrane capacitance were observed after 2 h of treatment with staurosporine, these results are included in **Fig. 4C**, which contains two plots of DEP spectra (untread cells vs. after 2h of treatment). From the DEP spectra it was identified that cytoplasmic conductivity decreased from 38 mS/m to 0.26 mS/m; while membrane capacitance also decreased from 38.7 mF/m^2 to 35.4 mF/m^2 (membrane conductance remained unchanged). The decrease in cytoplasmic conductivity agrees with the findings from studies performed with bacterial [35], yeast [45] and mammalian [6] cells. This study [59] also included Jurkat cells, for which the results were similar to those obtained with HeLA cells (a decrease on cytoplasmic conductivity and membrane capacitance). The findings from this work illustrate the significant progress on the use of DEP for studying apoptosis and cell death, as commercially available devices can now detect apoptosis much earlier than conventional methods. The Prasad group also studied apoptosis of cancer cells [66], they exposed non-small cell lung cancer (NSCLC) cells to the drug trypsin-EDTA navitoclax (ABT-263) and assessed cell response in an interdigitated electrode DEP system, which allowed them to detect changes in the physiological state of the cells as early as 2 h after cell exposure to ABT-263. The Chen and Wu group [67]

studied the effects of the anticancer drug doxorubicin (concentrations up to 15 μg/ml) on MES-SA cells, a human sarcoma cell line, employing an optical-induced DEP system. In their device, DEP effects were optically generated employing a beam of light that served as a virtual electrode array that enabled sorting the cells by moving them from the main channel to one of four distinct side channels, two channels located at each side of the main channel. They exploited differences in cell cytoplasm conductivity to sort the doxorubicin treated MES-SA cells into four groups according to their viability degrees. Their results revealed that 73.9 % of the MES-SA cells were dead after 48 h of treatment with doxorubicin at a concentration of 5 μg/ml, while only 4.5% of the cells with antidrug resistance were dead. This works demonstrated that DEP allows for effective sorting and separation of cells by exploiting changes in cell viability status. The Swami group extended their previous work on the effect of drugs on bacterial cell viability [35] to chemo-resistant circulating pancreatic cancer cells [68]. They developed a technology where single-cell cytometry was used to identify optimal frequencies to obtain a pDEP response of pancreatic ductal adenocarcinoma (PDAC) cells. The motivation of this work was the current challenges in enriching circulating tumor cells, which are present in low number in liquid biopsy samples. To this end, this study was focused on enriching live chemo-resistance PDAC cells, while rejecting dead cells, from an in vitro culture from metastatic tumor cells. They developed a device that enabled pDEP of live target cells that featured three distinct outlets, one outlet for each of the three DEP response types: pDEP, no DEP and nDEP. An additional challenge of this work was the fact that chemo-resistant PDAC cells have a wide size distribution that overlaps with other cell subpopulations in the sample (apoptotic and necrotic cells). Cell samples were treated with gemcitabine at a concentration of 1 μg/ml for 48 h prior to DEP assessments. Employing machine learning, the authors optimized the system and achieved effective enrichment of the live chemo-resistant PDAC cells from a sample containing only 3% of live cells to 44% at the pDEP outlet in their device in just 20 minutes, while rejecting 90% of the dead cells in the sample. The Kirby group [69] also investigated gemcitabine resistance of pancreatic cancer cells by developing a technique where EROT was used to obtain the cells' dielectric properties, which were then employed to predict DEP spectra that can be used for designing DEP-based separations between live and dead cells. These studies focused on the assessment of viability and apoptosis as a result of drug treatment on cancer cells have the potential to accelerate cancer treatment selection, while reducing cost and time.

The Lee group [70] separated live and heat-killed dead K562 cells, a human leukemia cell line, employing a novel device that integrated hydrodynamic focusing and DEP effects. An illustration of the device and the results obtained from the live dead separation process is shown in **Fig. 4D**. The device featured two electrode regions, the first one for focusing the cells and the second one for sorting the cells. A 3-dimensional narrow 20 μm constriction was located just prior to the focusing array of interdigitated electrodes to aide with the focusing process. A crucial aspect was to keep the cells close to the electrodes where DEP effects are effective. By carefully optimizing the cell-to-electrode distance and the frequency and voltage in each electrode region, the

continuous separation between live and dead K562 cells was achieved at a the very high rate > 150,000 cells/min, achieving a purity of 90% with a recovery of 85% of the live cells in the sample. As shown in **Fig. 4D**, live cells were sent to the collection outlet, while dead cells were sent to the waste outlet. The authors stated that they exploited the differences in membrane integrity between the live and dead cells, since the heat-killed K562 cells have a compromised cell membrane. A common theme is observed from the distinct reported discussed in this section, changes in cell membrane can be effectively exploited with DEP effects to achieve the sorting, separation and assessment of cancer cell viability status.

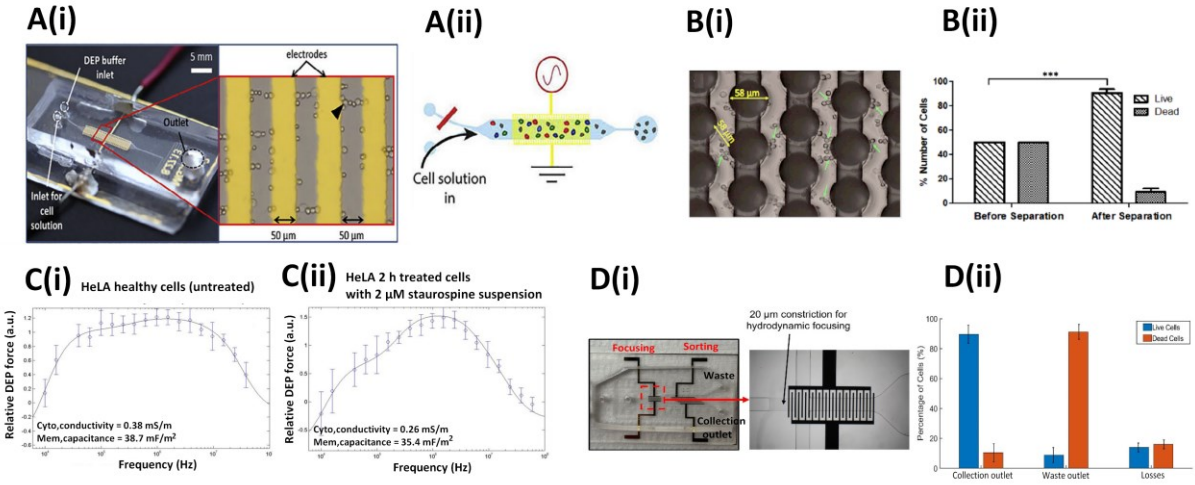

Fig. 4. Dielectrophoretic viability assessments of mammalian cells, blood cells and cancer cells. **(A.i)** Illustration of the large capacity electrode array employed by Adams et al. for the separation between live and dead NSPCs. **(A.ii)** Cartoon of the separation process, where live cells (red color) are selectively trapped by pDEP at the electrode array and dead cells (gray color) are flushed towards the outlet reservoir under Vpp at 1 MHz. Adapted with permission from [51], copyright (2018) Elsevier. **(B.i)** Image depicting live U937 monocytes trapped at the edges of the 3-dimensional carbon electrodes, the green arrows indicate trapping as pearl chain formations. **(B.ii)** B of the results from the separation of a 1:1 live dead mixture of live and dead monocytes, illustrating the enrichment of live monocytes after the separation. Adapted from [55], open access article under a Creative Commons Attribution License 4.0, copyright (2017) Yildizhan et al. **(C.i)** DEP spectra of HeLA untreaded cells and (C.ii) after 2 h of treatment with a 1 µM solution of staurosporine. DEP spectra was fitted using the single shell model and dielectric properties were extracted illustrating a decrease in both cytoplasmic conductivity and membrane capacitance. Adapted from [59] open access article under a Creative Commons Attribution-NonCommercial 3.0 Unported License, copyright (2016) Henslee et al. **(D.i)** Illustration of the device used by Aghaamoo et al., the left image depicts the entire device with two outlets and the right image shows in detail the interdigitated electrode array used to generate DEP effects. **(D.ii)** Plot of the live/dead cells sorting, where the majority of live cells (blue color) were sent at the collection outlet and the majority of dead cells were (orange color) sent to the waste outlet. Adapted from [70], open access article distributed under a Creative Commons Attribution (CC BY) License, copyright (2023) Aghaamoo et al.

3. Electrophoresis-based cell viability assessments and separations

Electrophoresis (EP), the migration of electrically charged particles (relative to a fluid) under the effects of an electric field, is a widely used technique in the analytical laboratory. In contrast with DEP that mainly operates under AC electric fields, EP is employed mainly with DC electric fields. There are a plethora of electrophoresis-based modes, including gel electrophoresis, the workhorse of analytical laboratory, and specialized modes such as zone electrophoresis, isotachophoresis, isoelectric focusing etc. Several research groups have reported effective EP-based separation techniques for the discrimination and separation between cells of distinct types

[16,71], there are also important reports exploring the origins of microbial electrical charge [72,73]. Despite these major advances, there is only a reduced number of EP-based studies focused on the assessment and separation between live and dead cells, which have been performed in bench scale CE systems and microfluidic systems. Described below are the operating principle and applications of EP designed specifically to distinguish and separate live from dead cells.

3.1 Electrophoresis operating principle

The fundamentals of traditional (linear) EP were developed mainly during the last century. The 20th century witnessed the major advancements in the understanding of the weak field theory. During this time, the techniques of gel EP and capillary electrophoresis (CE) became standards in the analytical laboratory [74]. The separation of cells by EP exploits differences in their electromigration velocity. The expression of the EP velocity under the weak field regime is defined as:

$$\mathbf{v}_{EP,L} = \mu_{EP,L}\mathbf{E} = \frac{\varepsilon_m \zeta_P}{\eta}\mathbf{E} \quad (3)$$

where $\mathbf{v}_{EP,L}$ refers to the linear electrophoretic velocity, $\mathbf{E}$ represents the electric field (where $\mathbf{E} = E\hat{\mathbf{a}}_E$ and $\hat{\mathbf{a}}_E$ is a unit vector with the direction of vector $\mathbf{E}$, having a magnitude of E). The parameter $\mu_{EP,L}$ is the mobility of linear EP and ζ_P is the electrokinetic (zeta) potential of the cell, ε_m and η represent the permittivity and viscosity of the suspending medium, respectively. The notation "L" in the linear electrophoretic velocity (and mobility) is used to distinguish it from the nonlinear electrophoretic velocity ($\mathbf{v}_{EP,NL}$) which will be discussed in this section. Since a large number of the systems used to assess and separate cells, namely CE or microchip electrophoresis, employ electroosmotic flow (EOF) for pumping the liquid and cells in the system, it is important to define the expression for the EOF velocity:

$$\mathbf{v}_{EO} = \mu_{EO}\mathbf{E} = -\frac{\varepsilon_m \zeta_W}{\eta}\mathbf{E} \quad (4)$$

where $\mathbf{v}_{EO}$ represents the EOF velocity and ζ_W is the zeta potential of the channel wall. The majority of EP-based separations reported in the literature are performed under the weak field regime, i.e., these reports exploit differences in electromigration velocity under linear EP (EP_L) effects [72,75–77]. Recent experimental reports [78–85] have unveiled the presence of a second EP effect, called nonlinear EP (EP_{NL}) or EP of the second kind, in EP-based separation systems. As discussed by Khair [11], major advances in the strong field theory have marked the last decade and have strengthened the understanding of EP_{NL}. Dukhin and collaborators first reported on the theory of EP_{NL} in the early 1970's [86], but widespread applications of EP^{NL} was delayed due to scarce availability of experimental data [87]. The importance of EP_{NL} in the separation of cells has been recently reported in microchip EP systems [88–91], and evidence of its effects on the electromigration of plastic nanoparticles has been characterized in CE systems [92]. Thus, EP_{NL} is an important effect that must be

considered in EP-based separations. The theory on EP_{NL} is still under development, and three dimensionless parameters: the dimensionless electric field (β), the Dukhin number (Du) and the Peclet number (Pe), are necessary for identifying the regimes of EP_{NL} [82]. The definitions of these three parameters are as follows:

$$\beta = \frac{E\, r_p}{\varphi}, \qquad Du = \frac{K^{\sigma}}{K^{m}\, r_p} \qquad \text{and} \qquad Pe = \frac{r_p |\mathbf{v}_{EP}|}{D} \tag{5}$$

where E is the electric field magnitude, r_p is the cell radius (hydrodynamic radius for non-spherical cells) and φ is the thermal voltage (~25 mV), In the expression for Du, K^{σ} and K^{m} are the surface conductivity and bulk conductivity of the medium, respectively. In the expression for Pe, $|\mathbf{v}_{EP}|$ is the magnitude of the electrophoretic velocity considering both linear and nonlinear contributions ($\mathbf{v}_{EP,L} + \mathbf{v}_{EP,NL}$) and D is the diffusion coefficient. The two following expressions for the velocity of EP_{NL} ($\mathbf{v}_{EP,NL}^{(n)}$) have been developed for the limiting cases of low Pe values ($Pe \ll 1$) and high Pe values ($Pe \gg 1$) [78,93,94]:

$$\mathbf{v}_{EP,NL}^{(3)} = \mu_{EP,NL}^{(3)} E^3 \hat{\mathbf{a}}_E \quad \text{for } \beta \leq 1, \text{ arbitrary } Du \text{ and } Pe \ll 1 \tag{6}$$

$$\mathbf{v}_{EP,NL}^{(3/2)} = \mu_{EP,NL}^{(3/2)} E^{3/2} \hat{\mathbf{a}}_E \text{ for } \beta > 1,\ Du \ll 1 \text{ and } Pe \gg 1 \tag{7}$$

where $\mu_{EP,NL}^{(n)}$ is the mobility of the EP_{NL} velocity and n represents the electric field dependence. As observed in **Eqns. (6-7)** the EP_{NL} velocity can have either a cubic or a 3/2 dependence (n = 3 or n = 3/2) with the electric field, as determined by values of β, Du and Pe. No analytical expressions for the EP_{NL} velocity are available yet for the intermediate values of Pe [78,93,94].

After introducing the main governing equations of EP, it is necessary to discuss how each regime of EP (EP_L and EP_{NL}) can differentiate between distinct types of cells, and for the purpose of this review article, how EP can differentiate between live and dead cells. First, EP-based separations can occur under DC and DC-biased low frequency AC electric fields, since under pure AC fields, EP effects, linear and nonlinear, cancel out and do not contribute to the separation process. Differences in electrical charge are effectively exploited with EP_L [11], as demonstrated by thousands of publications on CE [71,77,95]. Kłodzinska and Buszewski published an excellent article explaining the origins of microbial electrical charge [72]. However, EP_L cannot differentiate target analytes, such as live/dead cells, based on size or shape differences [96,97]. The use of EP_{NL} (**Eqns. 6-7**) is necessary to discriminate cells by size or shape differences [11,82,98]. In terms of the fundamental equations above, EP_L can discriminate between cells by differences in electrical charge (as determined by cell electrokinetic (zeta) potential in **Eqn. 1**, ζ_P), most microorganisms possess negative surface charge [73]. Differences in cell size and shape, which can be exploited by EP_{NL}, influence the values of the mobility of EP_{NL} ($\mu_{EP,NL}$), i.e., the values of $\mu_{EP,NL}$ depend on the size and shape of the cells [83,84,98]. However, due to the novelty of the application of EP_{NL} to discriminate between distinct cell types, there are no reports yet on the use of EP_{NL} for shape-based cell discriminations. A recent report from our group [89] demonstrated EP-based separations under linear and nonlinear modes. First, the separation of microparticles performed by exploiting

differences in electrical charge under EP_L was demonstrated, and second, the separation by exploiting differences in particle size under EP_{NL} was realized; resulting in a change of the elution order. Thus, the use of EP, linear and nonlinear mode, can enable effective separation schemes between viable and nonviable cells, since distinct parameters (charge, size or shape) can be exploited to achieve the desired separation, and switching between the linear and nonlinear modes of EP can be accomplished by simply modifying the magnitude of the applied electric voltage. Linear EP dominates the electromigration of cells at low electric fields, while EP_{NL} becomes a major effect on cell electromigration at high electric fields [89].

3.2 Reports on electrophoretic-based cell viability assessments and separations

Electrophoretic separations were first developed for large biological macromolecules, such as DNA and proteins [99]. The separation of intact cells by means of CE was first reported in 1987 by Hjertén *et al*. [100]. This was followed by the studies of Ebersole and McCormick [101] in 1983 and Armstrong *et al.* [102] in 1999. Armstrong in particular pioneered many of the first advances on the use of CE for separating intact microorganisms [102–104]. Numerous challenges, such as bacterial aggregation [105], undesired wall-cell interaction [72] and control of EOF [106] have been overcome during the last two decades. As data on the EP mobility became more available [107], contributions from the Buszewski [72,75,108] and Horká [109–111] research groups further established CE as technique with excellent capabilities for separating intact cells and observe the results as electropherograms. The recent knowledge on EP_{NL} [17], further confirms the potential of EP for separating viable and nonviable cells. However, only a handful of studies on the use of EP for cell viability assessments and separations have been reported. Below is a discussion on these studies and a summary of all the reports reviewed in this section is included in **Table 2**.

3.2.1 Bacteria cells

The first reports on an EP-based separation by exploiting differences in bacterial cell viability was reported in 2001 by the Armstrong group [112,113]. The authors stated that the motivation for their work was to illustrate the potential of EK-based separations (EP in this case) for the analysis and characterization of intact microorganisms, which is possible since all microbes have surface charge. They explained that microorganisms have membranes and cell walls that contain molecules such as proteins, lipids, lipopolysaccharides, teichoic acid, etc., which provide them with a characteristic surface electrical charge. This of course also depends on the characteristics of the suspending media, such as pH and ionic strength. The origins of surface charge on microorganisms have also been discussed on recent reports [72,73]. As reported by Polaczyk et al. [73], under physiological conditions, the majority of bacterial cells (and other types of cells) have a negative surface charge, which means that their EP migration will be towards the inlet (towards the anode), in the opposite direction of the EOF which is commonly towards the cathode in bare fused silica capillaries. The report by Polaczyk et al.

[73] listed only one case of a bacteria with a positive charge at pH values below 11 [114]. **Figure 5A** shows a cartoon of the migration of live and dead cells in an EP-based system. In this cartoon representation, both cell types, live and dead, have net negative surface charge, but dead cells have lower charge magnitude (lower magnitude of their negative ζ_P value), as reported in the literature [8,115].

In their first pioneer CE viability-based separation report [112], the Armstrong group assessed the quality of supplements for lactose intolerant individuals. They tested the live/dead cell content of *Lactobacillus acidophilus* (*L. acidophilus*) in tablets from food supplements. They employed a commercially available CE system with laser induced fluorescence (LIF) detection and were able to quantify the ratio of live to dead *L. acidophilus* cells in the sample as 60% of viable cells. However, no differences in the migration time of the live and dead cells were observed, the distinction and quantification of live cells was done employing the relative peak area of each type (live and dead) by assessing the fluorescence signal. The cells were fluorescently labeled employing propidium iodide for the dead cells and Syto 9 for the live cells. In their second pioneer CE viability study [113] the Armstrong group worked with cells samples of *L. acidophilus, Bifidobacterium infantis* (*B. infantis*) and *S. cerevisiae,* the bacteria were obtained from food supplements and the yeast from a freeze-dried supermarket product. Similar to their previous report [112], they employed CE-LIF and the same fluorescent dyes. The results showed that the peaks of the dead and live cells had almost identical migration times, and viability quantification was performed again by estimating the peak area employing fluorescence. Their viability determinations were 45%, 43% and <2% for *L. acidophilus, S. cerevisiae* and *B. infantis*, respectively. The analyzed the samples with flow cytometry, obtaining similar results (within the margin of error), illustrating that the CE-LIF viability determinations were accurate [113].

There have been important advances since these two pioneer CE cell viability reports from 2001 [112,113]. In 2017 Bonomo et al. [116] reported the separation of ethanol-stressed *Oenococcus oeni* (*O. oeni*) strains. They were interested in studying the viability changes caused by ethanol-induced environmental stress of the *O. oeni* cells, as these strains are important in wine production. Employing a CE system with a diode array detector, they were able to assess the changes on cell surface charge induced by the oxidative stress produced by alcohol exposure. They identified a large variability in the changes induced on the four distinct strains of *O. oeni* included in this study. In general, they observed from their CE analysis of the alcohol-treated samples that for each strain, at least three subpopulations were present, each population corresponding to a distinct electrical charge, as illustrated by three peaks: positive, neutral and negative charge peaks. Their results suggested that exposure to alcohol resulted in three types of cell viability status: injured, dormant and viable cells, corresponding to the positive, neutral and negative charge peaks, respectively. They observed, in general, that the subpopulation in the positive peak (damaged cells) increased with increased alcohol exposure. Similar results were obtained with flow cytometry, validating the CE analysis. The Buszewski group [117] recently published the CE-based viability analysis of five distinct strains of bacteria: *E. faecalis*, *S. aureus, Klebsiella pneumoniae*

(*K. pneumoniae*), *Pseudomonas aeruginosa* (*P. aeruginosa*) and *E. coli* which were treated with antibiotics. They analyzed three distinct samples of each strain: live untreaded cells, dead cells (inactivated with 70% ethanol) and antibiotic treated cells. A major goal of the study was to demonstrate the effect of antibiotics on the electrical charge and electromigration of cells. Their results, obtained with a capillary zone electrophoresis (CZE) system equipped with a diode array detector, are represented by the electropherogram for *E. faecalis* and the summary table contained in **Fig. 5B**. As seen from the electropherogram (**Fig. 5B.i**), dead and antibiotic-treated *E. faecalis* cells have a similar response in terms of their absorbance vs. time, but antibiotic-treated cells have slightly longer migration time than dead cells, while live cells have a longest migration time. The results in the table (**Fig. 5B.ii**) for all five cell strains follow the same trend, live cells have longer migration times than dead cells in the CZE system. These findings, which are in agreement with a previous report by the same group [115] and others [8,118,119], illustrate that dead bacterial cells have negative zeta potential values of lower magnitude than those of live cells. This causes live cells to have longer migration times, as they migrate behind dead cells (**Fig. 5A**). In a follow up study the Buszewski group [118] studied the effects of antibiotics on methicillin-resistant *S. aureus* (MRSA), methicillin-sensitive *S. aureus* (MSSA), and *E. coli*. Cells were treated with antibiotics for 24 h and dead cells were obtained by exposure to 70% ethanol. Similar results to their previous work [117] were obtained, dead cells had shorter migration times than live cells caused by their lower magnitude negative ζ_P values; while antibiotic-treated cells had an "intermediate" migration time, between those of dead and live cells. These results are illustrated in the electropherogram for *E. coli* cells in **Fig. 5C**. The viability results obtained with CE were compared with flow cytometry obtaining good agreement between the two methods. The authors stated that CE has the potential to become a routine method for cell viability assessments and separation in modern clinical practice [118].

More recently, our group separated live from dead *E. coli* cells employing a microchip EP system [119] which consisted of a T-shaped insulator-based (iEK) microfluidic channel that contained an array on cylindrical insulating pillars. The device employed and the results obtained are shown in **Fig. 5D**. For this separation the two phenomena of EP_L and EP_{NL}, described in **Section 3.1,** were employed. Our group has investigated extensively the use of EP_{NL} for the separation of cells and microparticles [32,88–91,98]. The presence of the insulating pillars in the iEK device in **Fig. 5D.i**. create regions of high electric field magnitude where nonlinear EK phenomena, such as EP_{NL} (and DEP to a lesser extent [88]) can arise and contribute to the separation process. Heat-treated dead cells and live cells were first characterized in terms of their ζ_P and $\mu_{EP,NL}^{(3)}$values, which were as follows: -25.5 ± 1.5 and -18.5 ± 0.8 mV for the ζ_P of live and dead cells, respectively; and -6.0 ± 0.6 and -3.0 ± 0.3 x10^{-18} $m^4V^{-3}s^{-1}$ for the $\mu_{EP,NL}^{(3)}$ of live and dead cells, respectively. For both EP phenomena, dead cells had a lower magnitude in both negative parameters, this means that EP effects on dead cells are lower than those for live cells, which agrees with several previous reports by other groups [8,115,118]. The values of

these parameters also indicated that engaging the nonlinear regime of EP will aid the separation, as it will increase the overall difference between live and dead cells. The electropherogram in **Fig. 5D.ii** illustrates a separation with a resolution of Rs = 1.87, where as expected, dead cells migrated ahead of live cells due to their lower EP effects (linear and nonlinear). The fluorescence signal from the cells was used to build the electropherogram, dead cells and live cells were labeled with propidium iodide and Syto 9 dyes, respectively. The employed iEK device and operating conditions could be further modified to increase the separation resolution as needed. A second objective of this study [119] was to re-analyze the results from a 2004 article [120] that reported the trapping at distinct locations of live and dead *E. coli* cells in an iEK device with cylindrical pillars. By leveraging the new knowledge on EP_{NL} it was possible to offer a new explanation on the results from the 2004 study; the trapping of live and dead *E.coli* cells shown in **Fig. 5E** are the results of EP_{NL} effects, and not DEP forces as it was originally assumed. The potential of EP-based systems for the separation and enrichment of bacterial cells based on cell viability status is significant, and the new knowledge on EP_{NL} opens novel and exciting possibilities.

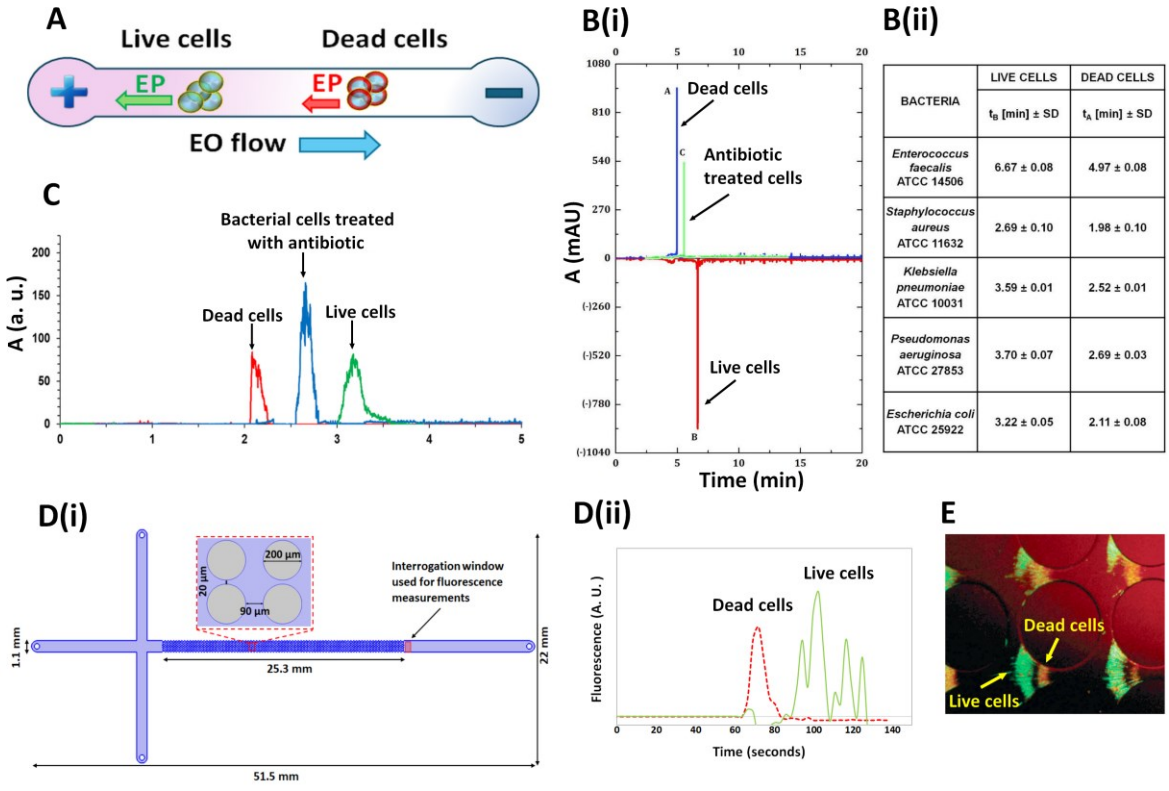

BACTERIA	LIVE CELLS	DEAD CELLS
	t_B [min] ± SD	t_A [min] ± SD
Enterococcus faecalis ATCC 14506	6.67 ± 0.08	4.97 ± 0.08
Staphylococcus aureus ATCC 11632	2.69 ± 0.10	1.98 ± 0.10
Klebsiella pneumoniae ATCC 10031	3.59 ± 0.01	2.52 ± 0.01
Pseudomonas aeruginosa ATCC 27853	3.70 ± 0.07	2.69 ± 0.03
Escherichia coli ATCC 25922	3.22 ± 0.05	2.11 ± 0.08

Fig. 5. Electrophoretic viability assessments of bacterial cells. **(A)** Cartoon illustration of the direction of EP migration and EOF in an electrophoretic system. It is important to note the opposite direction between EP migration and EOF. **(B.i)** CZE results as milli-absorbance unit (mAU) as a function of time obtained for E. *faecalis*. **(B.ii)** Summary table of migration times for live and dead (treated with 70% ethanol) bacterial cells. In all cases all dead cells have a shorter migration time than the live cells, indicating a lower magnitude of the cell negative zeta potential. Adapted from [117], open access article distributed under a Creative Commons Attribution (CC BY) License, copyright (2022) Kupczyk et al. **(C)** Electropherogram of dead, antibiotic-treat and live *E. coli* cells. Adapted with permission from [118], copyright (2022) John Wiley & Sons. (**D.i**) Illustration of the T-shaped iEK channel employed for the separation of live and dead *E. coli* cells. **(D.i)** Electropherogram of the separation of live and dead *E. coli* cells by exploiting linear and nonlinear EP effects.

Adapted from [119]. **(E)** Trapping of live (green) and dead (red) *E. coli* cells between the cylindrical insulating pillars in an iEK channel. Pillar diameter is 200 µm arranged in a 250 µm center-to-center square array. Adapted with permission from [120], copyright (2004) American Chemical Society.

3.2.1 Yeast cells

Similar to the advances with bacterial cells, the CE separation of *S. cerevisiae* cells based on cell viability was reported in 2016 by Crispo et al. [121] as a predecessor report from their work in 2017 with *O. oeni* bacterial strains [116]. To separate live and dead *S. cerevisiae* cells by means of CZE with a diode array detector (DAD), dead cells were prepared by thermal treatment. The live/dead cell separation, performed after optimizing the CZE separation conditions, resulted in an electropherogram with two distinct peaks, which illustrated the presence of two cell subpopulations (as also observed in their latter report [116]). They identified that heat-treated dead *S. cerevisiae* cell had almost no electrical charge and eluted ahead of live negatively-charged cells. An interesting observation was that the dead cell peak (uncharged cells) was better defined than the peak corresponding to live cells, they explained these results as dead cells being more homogeneous in size than live cells. This separation took less than 5 minutes as shown in the electropherogram in **Fig. 6**. Similarly to the studies on EP-separation of bacterial cells, this report contributes to the growing evidence that simple EP-based systems are effective options for the rapid separation and assessment of live and dead yeast cells.

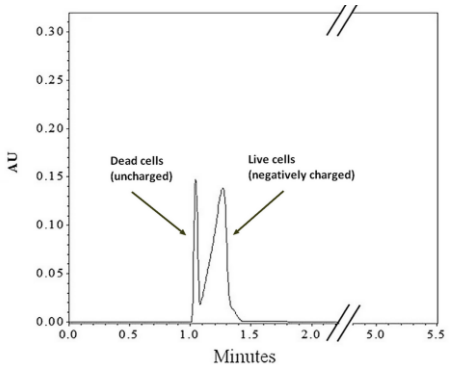

Fig. 6. Electrophoretic viability assessments of yeast cells. Electropherogram of the separation between live and dead S. cerevisiae cells by CZE. Dead cells, which are uncharged eluted ahead of live cells. Adapted with permission from [121], copyright (2016) Elsevier.

4. Concluding remarks

The rapid assessment of cell viability status is essential in several fields, including clinical analysis, drug development, food safety and quality control, among others. In numerous applications the sorting and separation of live and dead cells is also required, as further analysis can be performed with separated fractions of viable and nonviable cells. Electrokinetic phenomena, being robust and label-free, offer great potential as techniques for the simultaneous assessment and separation of cells based on their viability status. This review article discusses the fundamentals, presents a brief historical overview and analyzes relevant recent (2015-2024) reports on two

electrokinetics techniques that can assess and separate cells based on viability status; these techniques are dielectrophoresis and electrophoresis. The similarities and differences of both techniques are examined. Dielectrophoresis discriminates live from dead cells by differences in polarizability, where in the majority of the studies live cells exhibited positive dielectrophoresis and dead cells exhibited negative dielectrophoresis, these differences enables effective live/dead cell sorting. Electrophoresis, in contrast, exploits differences in electromigration velocity (which is dictated by cell electrical charge, size and shape), and viable cells are separated from nonviable ones in the form of two different zones inside the capillary/microchannel manifested as two resolved peaks on the electropherogram. A detailed discussion on very recent developments on nonlinear electrophoresis is also included, to provide the reader with the most up-to-date advances and showcase the new capabilities of electrophoresis-based separation systems. The field of electrokinetics, although not new, is still rapidly evolving and novel studies are continuously being reported. It is expected that new developments will further increase the viability-based discriminatory capabilities of both techniques. Perhaps viability assessments and separations with electrophoresis can be extended to mammalian and cancer cells in the future.

Declaration of Competing Interest

The author declares no competing financial interest.

Author contributions: CRediT

BHLE: Conceptualization, Funding acquisition, Project administration, Writing Original Draft – Review & Editing.

Data availability

Data sharing is not applicable to this article as no new data were created or analyzed in this study.

Acknowledgments

This material is based upon work supported by the National Science Foundation under Awards No. 2127592 and No. 2133207. The authors acknowledge Research Computing at the Rochester Institute of Technology for providing computational resources and support that have contributed to the research results reported in this publication.

ORCID

Blanca H. Lapizco-Encinas: 0000-0001-6283-8210

References

[1] M.P.. William A. Rutala, Ph.D., Guideline for disinfection and sterilization in healthcare facilities: Updated 2017, Healthc. Infect. Control Pract. Advis. Comm. (2017) 1–158. https://stacks.cdc.gov/view/cdc/47378 (accessed February 2, 2024).

[2] S.A. Alali, E. Shrestha, A.R. Kansakar, A. Parekh, S. Dadkhah, W.F. Peacock, Community hospital stethoscope cleaning practices and contamination rates, Am. J. Infect. Control. 48 (2020) 1365–1369. https://doi.org/10.1016/j.ajic.2020.04.019.

[3] G.F. Hatfull, R.M. Dedrick, R.T. Schooley, Phage Therapy for Antibiotic-Resistant Bacterial Infections, Annu. Rev. Med. 73 (2022) 197–211. https://doi.org/10.1146/annurev-med-080219-122208.

[4] S. He, Y. Chen, J. Wang, J. Sun, X. Zhang, Q. Chen, Rapid and Sensitive Quantification of Bacterial Viability Using Ratiometric Fluorescence Sensing, Anal. Chem. (2024). https://doi.org/10.1021/ACS.ANALCHEM.4C01737.

[5] M. Puiu, C. Bala, Microfluidics-integrated biosensing platforms as emergency tools for on-site field detection of foodborne pathogens, TrAC - Trends Anal. Chem. 125 (2020). https://doi.org/10.1016/j.trac.2020.115831.

[6] S. Afshar, E. Salimi, A. Fazelkhah, K. Braasch, N. Mishra, M. Butler, D.J. Thomson, G.E. Bridges, Progression of change in membrane capacitance and cytoplasm conductivity of cells during controlled starvation using dual-frequency DEP cytometry, Anal. Chim. Acta. 1059 (2019) 59–67. https://doi.org/10.1016/j.aca.2019.01.046.

[7] B. Larbi, A. Ltaief, A. Hawari, F. Du, M. Baune, J. Thöming, Assessment of the Effect of Dielectrophoresis (DEP) on the Viability of Activated Sludge Biomass, Int. J. Environ. Sci. Dev. 8 (2017) 715–718. https://doi.org/10.18178/ijesd.2017.8.10.1044.

[8] B.D. Ho, J.P. Beech, J.O. Tegenfeldt, Cell sorting using electrokinetic deterministic lateral displacement, Micromachines. 12 (2021) 1–14. https://doi.org/10.3390/mi12010030.

[9] C.I. Trainito, E. Bayart, E. Bisceglia, F. Subra, O. Français, B. Le Pioufle, Electrorotation as a versatile tool to estimate dielectric properties of multi-scale biological samples: From single cell to spheroid analysis, IFMBE Proc. 53 (2016) 75–78. https://doi.org/10.1007/978-981-287-817-5_17.

[10] B.H. Lapizco-Encinas, Microscale nonlinear electrokinetics for the analysis of cellular materials in clinical applications: a review, Microchim. Acta. 188 (2021) 104. https://doi.org/10.1007/s00604-021-04748-7.

[11] A.S. Khair, Nonlinear electrophoresis of colloidal particles, Curr. Opin. Colloid Interface Sci. 59 (2022) 101587. https://doi.org/10.1016/j.cocis.2022.101587.

[12] J. Zhang, Z. Song, Q. Liu, Y. Song, Recent advances in dielectrophoresis-based cell viability assessment, Electrophoresis. 41 (2020) 917–932. https://doi.org/10.1002/elps.201900340.

[13] E.A. Henslee, Review: Dielectrophoresis in cell characterization, Electrophoresis. 41 (2020) 1915–1930. https://doi.org/10.1002/elps.202000034.

[14] A.R. Hyler, D. Hong, R. V. Davalos, N.S. Swami, E.M. Schmelz, A novel ultralow conductivity electromanipulation buffer improves cell viability and enhances dielectrophoretic consistency, Electrophoresis. 42 (2021) 1366–1377. https://doi.org/10.1002/elps.202000324.

[15] Z. Çağlayan, Y. Demircan Yalçın, H. Külah, A Prominent Cell Manipulation Technique in BioMEMS: Dielectrophoresis, Micromachines. 11 (2020) 990. https://doi.org/10.3390/mi11110990.

[16] A. Vaghef-Koodehi, B.H. Lapizco-Encinas, Microscale electrokinetic-based analysis of intact cells and viruses, Electrophoresis. 43 (2022) 263–287. https://doi.org/10.1002/elps.202100254.

[17] B.H. Lapizco-Encinas, Nonlinear Electrokinetic Methods of Particles and Cells, Annu. Rev. Anal. Chem. 17 (2024) 243–264. https://doi.org/10.1146/annurev-anchem-061622-040810.

[18] R. Deivasigamani, N.N. Mohd Maidin, N.S. Abdul Nasir, A. Abdulhameed, A. Bin Ahmad Kayani, M.A. Mohamed, M.R. Buyong, A correlation of conductivity medium and bioparticle viability on dielectrophoresis-based biomedical applications, Electrophoresis. 44 (2023) 573–620. https://doi.org/10.1002/elps.202200203.

[19] M. Punjiya, H.R. Nejad, J. Mathews, M. Levin, S. Sonkusale, A flow through device for simultaneous dielectrophoretic cell trapping and AC electroporation, Sci. Rep. 9 (2019) 1–11. https://doi.org/10.1038/s41598-019-48198-x.

[20] M.P. Hughes, Fifty years of dielectrophoretic cell separation technology, Biomicrofluidics. 10 (2016). https://doi.org/10.1063/1.4954841.

[21] K. Zhao, Larasati, B.P. Duncker, D. Li, Continuous Cell Characterization and Separation by Microfluidic Alternating Current Dielectrophoresis, Anal. Chem. 91 (2019) 6304–6314. https://doi.org/10.1021/acs.analchem.9b01104.

[22] P. Patel, G.H. Markx, Dielectric measurement of cell death, Enzyme Microb. Technol. 43 (2008) 463–470. https://doi.org/10.1016/j.enzmictec.2008.09.005.

[23] H.A. Pohl, The Motion and Precipitation of Suspensoids in Divergent Electric Fields, J. Appl. Phys. 22 (1951) 869–871.

[24] H.A. Pohl, I. Hawk, Separation of living and dead cells by dielectrophoresis, Science (80-.). 152 (1966) 647–649. https://doi.org/10.1126/science.152.3722.647-a.

[25] J.S. Crane, H.A. Pohl, A study of living and dead yeast cells using dielectrophoresis, J. Electrochem. Soc. 115 (1968) 584–586. https://doi.org/10.1149/1.2411345.

[26] M.A. Saucedo-Espinosa, A. Lalonde, A. Gencoglu, M.F. Romero-Creel, J.R. Dolas, B.H. Lapizco-Encinas, Dielectrophoretic manipulation of particle mixtures employing asymmetric insulating posts, Electrophoresis. 37 (2016) 282–290. https://doi.org/10.1002/elps.201500195.

[27] P.A. Zellner, A. Sahari, Y. Hosseini, B. Behkam, M. Agah, Selective E. coli trapping with 3D insulator-based dielectrophoresis using DC-biased, AC electric fields, in: Proc. Annu. Int. Conf. IEEE Eng. Med. Biol. Soc. EMBS, 2012: pp. 6285–6288. https://doi.org/10.1109/EMBC.2012.6347431.

[28] D. Nakidde, P. Zellner, M.M. Alemi, T. Shake, Y. Hosseini, M. V. Riquelme, A. Pruden, M. Agah, Three dimensional passivated-electrode insulator-based dielectrophoresis, Biomicrofluidics. 9 (2015) 14125. https://doi.org/10.1063/1.4913497.

[29] P. Zellner, T. Shake, Y. Hosseini, D. Nakidde, M. V. Riquelme, A. Sahari, A. Pruden, B. Behkam, M. Agah, 3D Insulator-based dielectrophoresis using DC-biased, AC electric fields for selective bacterial trapping, Electrophoresis. 36 (2015) 277–283. https://doi.org/10.1002/elps.201400236.

[30] K. Kikkeri, M.V. Riquelme Breazeal, X. Ren, A. Pruden, M. Agah, A Monolithic Dielectrophoresis Chip with Impedimetric Sensing for Assessment of Pathogen Viability, J. Microelectromechanical Syst. 27 (2018) 810–817. https://doi.org/10.1109/JMEMS.2018.2860926.

[31] B. Ho, J. Beech, J. Tegenfeldt, Charge-Based Separation of Micro- and Nanoparticles, Micromachines. 11 (2020) 1014. https://doi.org/10.3390/mi11111014.

[32] A. Vaghef-Koodehi, C. Dillis, B.H. Lapizco-Encinas, High-Resolution Charge-Based Electrokinetic Separation of Almost Identical Microparticles, Anal. Chem. 94 (2022) 6451–6456. https://doi.org/10.1021/acs.analchem.2c00355.

[33] Y.H. Su, C.A. Warren, R.L. Guerrant, N.S. Swami, Dielectrophoretic monitoring and interstrain separation of intact clostridium difficile based on their S(Surface)-layers, Anal. Chem. 86 (2014) 10855–10863. https://doi.org/10.1021/ac5029837.

[34] Y.H. Su, A. Rohani, C.A. Warren, N.S. Swami, Tracking Inhibitory Alterations during Interstrain Clostridium difficile Interactions by Monitoring Cell Envelope Capacitance, ACS Infect. Dis. 2 (2016) 544–551. https://doi.org/10.1021/acsinfecdis.6b00050.

[35] A. Rohani, J.H. Moore, Y.H. Su, V. Stagnaro, C. Warren, N.S. Swami, Single-cell electro-phenotyping for rapid assessment of Clostridium difficile heterogeneity under vancomycin treatment at sub-MIC (minimum inhibitory concentration) levels, Sensors Actuators, B Chem. 276 (2018) 472–480. https://doi.org/10.1016/j.snb.2018.08.137.

[36] M. Goel, A. Verma, S. Gupta, Electric-field driven assembly of live bacterial cell microarrays for rapid phenotypic assessment and cell viability testing, Biosens. Bioelectron. 111 (2018) 159–165. https://doi.org/10.1016/j.bios.2018.04.005.

[37] P. Swami, A. Sharma, S. Anand, S. Gupta, DEPIS: A combined dielectrophoresis and impedance spectroscopy platform for rapid cell viability and antimicrobial susceptibility analysis, Biosens. Bioelectron. 182 (2021) 113190. https://doi.org/10.1016/j.bios.2021.113190.

[38] S. Pudasaini, A.T.K. Perera, D. Das, S.H. Ng, C. Yang, Continuous flow microfluidic cell inactivation

with the use of insulating micropillars for multiple electroporation zones, Electrophoresis. 40 (2019) 2522–2529. https://doi.org/10.1002/elps.201900150.

[39] S. Pudasaini, A.T.K. Perera, S.S.U. Ahmed, Y.B. Chong, S.H. Ng, C. Yang, An electroporation device with microbead-enhanced electric field for bacterial inactivation, Inventions. 5 (2020) 2. https://doi.org/10.3390/inventions5010002.

[40] S. Pudasaini, A.T.K. Perera, S.H. Ng, C. Yang, Bacterial inactivation via microfluidic electroporation device with insulating micropillars, Electrophoresis. 42 (2021) 1093–1101. https://doi.org/10.1002/elps.202000326.

[41] Y. Mizuta, H. Takuya, T.D. Nguyen, K. Taguchi, Cell Fusion and Distinction between Viable Cell and Non-Viable Cell Using Dielectrophoresis and Optical Tweezers, in: Proc. 2015 Int. Conf. Electr. Autom. Mech. Eng., 2015: pp. 59–62. https://doi.org/10.2991/eame-15.2015.16.

[42] R. Komai, K. Aritoshi, K. Taguchi, Efficient Evaluation Method of Cell's Viability Using Dielectrophoresis, Appl. Mech. Mater. 870 (2017) 375–379. https://doi.org/10.4028/www.scientific.net/amm.870.375.

[43] F.-J. Garcia-Diego, M. Rubio-Chavarria, P. Beltran, F.J. Espinos, G.-D. Fernando-Juan, M. Rubio-Chavarría, P. Beltrán, F.J. Espinós, Thermal Shock Response of Yeast Cells Characterised by Dielectrophoresis Force Measurement, Sensors. 19 (2019) 5304. https://doi.org/10.3390/s19235304.

[44] H.M. Ettehad, P.S. Zarrin, R. Hölzel, C. Wenger, Dielectrophoretic immobilization of yeast cells using CMOS integrated microfluidics, Micromachines. 11 (2020) 501. https://doi.org/10.3390/MI11050501.

[45] H.M. Ettehad, C. Wenger, Characterization and separation of live and dead yeast cells using cmos-based dep microfluidics, Micromachines. 12 (2021) 270. https://doi.org/10.3390/mi12030270.

[46] Y. Wu, R. Chattaraj, Y. Ren, H. Jiang, D. Lee, Label-Free Multitarget Separation of Particles and Cells under Flow Using Acoustic, Electrophoretic, and Hydrodynamic Forces, Anal. Chem. 93 (2021) 7635–7646. https://doi.org/10.1021/acs.analchem.1c00312.

[47] S. Bunthawin, P. Srichan, K. Jaruwongrungsee, R.J. Ritchie, Using dielectrophoretic spectra to identify and separate viable yeast cells, Appl. Microbiol. Biotechnol. 107 (2023) 7647–7655. https://doi.org/10.1007/s00253-023-12809-5.

[48] S. Afshar, E. Salimi, K. Braasch, M. Butler, D. Thomson, G. Bridges, Two-frequency dielectrophoresis analysis of viable/non-viable single CHO cells employing a microwave cytometer, in: BioWireleSS 2016 - Proceedings, 2016 IEEE Top. Conf. Biomed. Wirel. Technol. Networks, Sens. Syst., IEEE, 2016: pp. 70–73. https://doi.org/10.1109/BIOWIRELESS.2016.7445565.

[49] E. Salimi, K. Braasch, A. Fazelkhah, S. Afshar, B. Saboktakin Rizi, K. Mohammad, M. Butler, G.E. Bridges, D.J. Thomson, Single cell dielectrophoresis study of apoptosis progression induced by controlled starvation, Bioelectrochemistry. 124 (2018) 73–79.

https://doi.org/10.1016/j.bioelechem.2018.07.003.
[50] S. Afshar, A. Fazelkhah, E. Salimi, M. Butler, D. Thomson, G. Bridges, In-Flow Dielectrophoresis Sensor for Measuring the Dielectric Spectrum of Single Cells: Viable and Non-viable Cells, Proc. IEEE Sensors. 2019-Octob (2019) 1–4. https://doi.org/10.1109/SENSORS43011.2019.8956709.
[51] T.N.G. Adams, A.Y.L. Jiang, P.D. Vyas, L.A. Flanagan, Separation of neural stem cells by whole cell membrane capacitance using dielectrophoresis, Methods. 133 (2018) 91–103. https://doi.org/10.1016/j.ymeth.2017.08.016.
[52] R. Natu, M. Islam, D. Keck, R. Martinez-Duarte, Automated “pick and transfer” of targeted cells using dielectrophoresis, Lab Chip. 19 (2019) 2512–2525. https://doi.org/10.1039/c9lc00409b.
[53] A.J. Smith, R.D. O’Rorke, A. Kale, R. Rimsa, M.J. Tomlinson, J. Kirkham, A.G. Davie, C. Wälti, C.D. Wood, Rapid cell separation with minimal manipulation for autologous cell therapies, Sci. Rep. 7 (2017) 1–15. https://doi.org/10.1038/srep41872.
[54] K. Torres-Castro, C. Honrado, W.B. Varhue, V. Farmehini, N.S. Swami, High-throughput dynamical analysis of dielectrophoretic frequency dispersion of single cells based on deflected flow streamlines, Anal. Bioanal. Chem. 412 (2020) 3847–3857. https://doi.org/10.1007/s00216-020-02467-1.
[55] Y. Yildizhan, N. Erdem, M. Islam, R. Martinez-Duarte, M. Elitas, Dielectrophoretic separation of live and dead monocytes using 3D carbon-electrodes, Sensors. 17 (2017) 2691. https://doi.org/10.3390/s17112691.
[56] V.D. Jayasooriya, D. Nawarathna, Label-free purification of viable human T-lymphocyte cells from a mixture of viable and non-viable cells after transfection by electroporation, J. Phys. D. Appl. Phys. 52 (2019) 36LT01. https://doi.org/10.1088/1361-6463/ab2b81.
[57] A. Mustafa, E. Pedone, L. Marucci, D. Moschou, M. Di Lorenzo, A flow-through microfluidic chip for continuous dielectrophoretic separation of viable and non-viable human T-cells, Electrophoresis. 43 (2022) 501–508. https://doi.org/10.1002/elps.202100031.
[58] V. Jayasooriya, D. Nawarathna, Design of Micro-interdigitated Electrodes and Detailed Impedance Data Analysis for Label-free Biomarker Quantification, Electroanalysis. 29 (2017) 330–338. https://doi.org/10.1002/elan.201600364.
[59] E.A. Henslee, R.M. Torcal Serrano, F.H. Labeed, R.I. Jabr, C.H. Fry, M.P. Hughes, K.F. Hoettges, Accurate quantification of apoptosis progression and toxicity using a dielectrophoretic approach, Analyst. 141 (2016) 6408–6415. https://doi.org/10.1039/c6an01596d.
[60] M. Sun, P. Agarwal, S. Zhao, Y. Zhao, X. Lu, X. He, Continuous on-chip cell separation based on conductivity-induced dielectrophoresis with 3D self-assembled ionic liquid electrodes, Anal. Chem. 88 (2016) 8264–8271. https://doi.org/10.1021/acs.analchem.6b02104.
[61] X. Wang, F.F. Becker, P.R.C. Gascoyne, Membrane dielectric changes indicate induced apoptosis in HL-

60 cells more sensitively than surface phosphatidylserine expression or DNA fragmentation, Biochim. Biophys. Acta - Biomembr. 1564 (2002) 412–420. https://doi.org/10.1016/S0005-2736(02)00495-9.

[62] S. Mahabadi, F.H. Labeed, M.P. Hughes, Dielectrophoretic analysis of treated cancer cells for rapid assessment of treatment efficacy, Electrophoresis. 39 (2018) 1104–1110. https://doi.org/10.1002/elps.201700488.

[63] M.P. Hughes, F.H. Labeed, K.F. Hoettges, S. Porter, V. Mercadante, N. Kalavrezos, C. Liew, J.A. McCaul, R. Kulkarni, J. Cymerman, C. Kerawala, J. Barber, M.P. Lewis, S. Fedele, Point-of-care Analysis for Non-invasive Diagnosis of Oral cancer (PANDORA): A technology-development proof of concept diagnostic accuracy study of dielectrophoresis in patients with oral squamous cell carcinoma and dysplasia, J. Oral Pathol. Med. 52 (2023) 305–314. https://doi.org/10.1111/jop.13417.

[64] E.D. Lavi, F. Crivellari, Z. Gagnon, Dielectrophoretic detection of electrical property changes of stored human red blood cells, Electrophoresis. 43 (2022) 1297–1308. https://doi.org/10.1002/elps.202100241.

[65] K.F. Hoettges, E.A. Henslee, R.M. Torcal Serrano, R.I. Jabr, R.G. Abdallat, A.D. Beale, A. Waheed, P. Camelliti, C.H. Fry, D.R. van der Veen, F.H. Labeed, M.P. Hughes, Ten–Second Electrophysiology: Evaluation of the 3DEP Platform for high-speed, high-accuracy cell analysis, Sci. Rep. 9 (2019) 19153. https://doi.org/10.1038/s41598-019-55579-9.

[66] R. Taruvai Kalyana Kumar, S. Liu, J.D. Minna, S. Prasad, Monitoring drug induced apoptosis and treatment sensitivity in non-small cell lung carcinoma using dielectrophoresis, Biochim. Biophys. Acta - Gen. Subj. 1860 (2016) 1877–1883. https://doi.org/10.1016/j.bbagen.2016.05.039.

[67] P.Y. Chu, C.J. Liao, C.H. Hsieh, H.M. Wang, W.P. Chou, P.H. Chen, M.H. Wu, Utilization of optically induced dielectrophoresis in a microfluidic system for sorting and isolation of cells with varied degree of viability: Demonstration of the sorting and isolation of drug-treated cancer cells with various degrees of anti-cancer dru, Sensors Actuators B Chem. 283 (2019) 621–631. https://doi.org/10.1016/J.SNB.2018.12.047.

[68] A. Rane, J. Jarmoshti, A.-B. Siddique, S. Adair, K. Torres-Castro, C. Honrado, T.W. Bauer, N.S. Swami, Dielectrophoretic enrichment of live chemo-resistant circulating-like pancreatic cancer cells from media of drug-treated adherent cultures of solid tumors., Lab Chip. 24 (2024) 561–571. https://doi.org/10.1039/d3lc00804e.

[69] T. Lannin, W.W. Su, C. Gruber, I. Cardle, C. Huang, F. Thege, B. Kirby, Automated electrorotation shows electrokinetic separation of pancreatic cancer cells is robust to acquired chemotherapy resistance, serum starvation, and EMT, Biomicrofluidics. 10 (2016). https://doi.org/10.1063/1.4964929.

[70] M. Aghaamoo, B. Cardenas-Benitez, A.P. Lee, A High-Throughput Microfluidic Cell Sorter Using a Three-Dimensional Coupled Hydrodynamic-Dielectrophoretic Pre-Focusing Module, Micromachines. 14 (2023) 1813. https://doi.org/10.3390/mi14101813.

[71] B. Buszewski, E. Kłodzińska, Rapid microbiological diagnostics in medicine using electromigration techniques, TrAC - Trends Anal. Chem. 78 (2016) 95–108. https://doi.org/10.1016/j.trac.2016.02.008.

[72] E. Kłodzińska, B. Buszewski, Electrokinetic detection and characterization of intact microorganisms, Anal. Chem. 81 (2009) 8–15. https://doi.org/10.1021/ac801369a.

[73] A.L. Polaczyk, J.E. Amburgey, A. Alansari, J.C. Poler, M. Propato, V.R. Hill, Calculation and uncertainty of zeta potentials of microorganisms in a 1:1 electrolyte with a conductivity similar to surface water, Colloids Surfaces A Physicochem. Eng. Asp. 586 (2020) 124097. https://doi.org/10.1016/j.colsurfa.2019.124097.

[74] P.G. Righetti, 50, 100, 1000 Years: Happy Anniversary Electrophoresis!, Electrophoresis. 40 (2019) 11–15. https://doi.org/10.1002/elps.201800447.

[75] B. Buszewski, M. Szumski, E. Kłodzińska, H. Dahm, Separation of bacteria by capillary electrophoresis, J. Sep. Sci. 26 (2003) 1045–1049. https://doi.org/10.1002/jssc.200301442.

[76] A. Rogowska, P. Pomastowski, M. Złoch, V. Railean-Plugaru, A. Król, K. Rafińska, M. Szultka-Młyńska, B. Buszewski, The influence of different pH on the electrophoretic behaviour of Saccharomyces cerevisiae modified by calcium ions, Sci. Rep. 8 (2018) 7261. https://doi.org/10.1038/s41598-018-25024-4.

[77] B. Buszewski, E. Maślak, M. Złoch, V. Railean-Plugaru, E. Kłodzińska, P. Pomastowski, A new approach to identifying pathogens, with particular regard to viruses, based on capillary electrophoresis and other analytical techniques, TrAC - Trends Anal. Chem. 139 (2021). https://doi.org/10.1016/J.TRAC.2021.116250.

[78] M. Rouhi Youssefi, F.J. Diez, Ultrafast electrokinetics, Electrophoresis. 37 (2016) 692–698. https://doi.org/10.1002/elps.201500392.

[79] S. Tottori, K. Misiunas, U.F. Keyser, D.J. Bonthuis, Nonlinear Electrophoresis of Highly Charged Nonpolarizable Particles, Phys. Rev. Lett. 123 (2019) 14502. https://doi.org/10.1103/PhysRevLett.123.014502.

[80] B. Cardenas-Benitez, B. Jind, R.C. Gallo-Villanueva, S.O. Martinez-Chapa, B.H. Lapizco-Encinas, V.H. Perez-Gonzalez, Direct Current Electrokinetic Particle Trapping in Insulator-Based Microfluidics: Theory and Experiments, Anal. Chem. 92 (2020) 12871–12879. https://doi.org/10.1021/acs.analchem.0c01303.

[81] S. Antunez-Vela, V.H. Perez-Gonzalez, A. Coll De Peña, C.J. Lentz, B.H. Lapizco-Encinas, Simultaneous Determination of Linear and Nonlinear Electrophoretic Mobilities of Cells and Microparticles, Anal. Chem. 92 (2020) 14885–14891. https://doi.org/10.1021/acs.analchem.0c03525.

[82] J. Bentor, H. Dort, R.A. Chitrao, Y. Zhang, X. Xuan, Nonlinear electrophoresis of dielectric particles in Newtonian fluids, Electrophoresis. 44 (2023) 938–946. https://doi.org/10.1002/elps.202200213.

[83] J. Bentor, X. Xuan, Nonlinear electrophoresis of nonspherical particles in a rectangular microchannel, Electrophoresis. (2023). https://doi.org/10.1002/ELPS.202300188.

[84] V. Kasarabada, O.D. Ernst, A. Vaghef-Koodehi, B.H. Lapizco-Encinas, Effect of cell shape on nonlinear electrophoresis migration, J. Chromatogr. A. 1717 (2024) 464685. https://doi.org/10.1016/j.chroma.2024.464685.

[85] E. Frants, S. Amiroudine, E. Demekhin, DNS of Nonlinear Electrophoresis, Microgravity Sci. Technol. 36 (2024) 1–22. https://doi.org/10.1007/s12217-024-10108-w.

[86] S.S. Dukhin, Electrokinetic phenomena of the second kind and their applications, Adv. Colloid Interface Sci. 35 (1991) 173–196. https://doi.org/10.1016/0001-8686(91)80022-C.

[87] N.A. Mishchuk, N.O. Barinova, Theoretical and experimental study of nonlinear electrophoresis, Colloid J. 73 (2011) 88–96. https://doi.org/10.1134/S1061933X11010133.

[88] A. Vaghef-Koodehi, O.D. Ernst, B.H. Lapizco-Encinas, Separation of Cells and Microparticles in Insulator-Based Electrokinetic Systems, Anal. Chem. 95 (2023) 1409–1418. https://doi.org/10.1021/acs.analchem.2c04366.

[89] A. Vaghef-Koodehi, B.H. Lapizco-Encinas, Switching Separation Migration Order by Switching Electrokinetic Regime in Electrokinetic Microsystems, Biosens. 2024, Vol. 14, Page 119. 14 (2024) 119. https://doi.org/10.3390/BIOS14030119.

[90] N.N. Nasir Ahamed, C.A. Mendiola-Escobedo, V.H. Perez-Gonzalez, B.H. Lapizco-Encinas, Development of a DC-biased AC stimulated microfluidic device for the electrokinetic separation of bacterial and yeast cells, Biosensors. 14 (2024) 237. https://doi.org/10.3390/BIOS14050237.

[91] N.N. Nasir Ahamed, C.A. Mendiola-Escobedo, V.H. Perez-Gonzalez, B.H. Lapizco-Encinas, Assessing the Discriminatory Capabilities of iEK Devices under DC and DC-Biased AC Stimulation Potentials, Micromachines. 14 (2023). https://doi.org/10.3390/mi14122239.

[92] C. Adelantado, B.H. Lapizco-Encinas, J. Jordens, S. Voorspoels, M. Velimirovic, K. Tirez, Capillary Electrophoresis as a Complementary Analytical Tool for the Separation and Detection of Nanoplastic Particles, Anal. Chem. 96 (2024) 7706–7713. https://doi.org/10.1021/acs.analchem.4c00822.

[93] E. Yariv, O. Schnitzer, The electrophoretic mobility of rod-like particles, J. Fluid Mech. 719 (2013) 1–12. https://doi.org/10.1017/jfm.2013.43.

[94] O. Schnitzer, E. Yariv, Nonlinear electrophoresis at arbitrary field strengths: Small-Dukhin-number analysis, Phys. Fluids. 26 (2014) 122002. https://doi.org/10.1063/1.4902331.

[95] F. Krebs, H. Zagst, M. Stein, R. Ratih, R. Minkner, M. Olabi, S. Hartung, C. Scheller, B.H. Lapizco-Encinas, C. Sänger-van de Griend, C.D. García, H. Wätzig, Strategies for capillary electrophoresis: Method development and validation for pharmaceutical and biological applications—Updated and completely revised edition, Electrophoresis. 44 (2023) 1279–1341.

https://doi.org/10.1002/elps.202300158.
[96] D. Li, Chapter 9 - Electrophoretic motion of particles in microchannels, in: Interface Sci. Technol., 2004: pp. 542–616. https://doi.org/10.1016/S1573-4285(04)80031-0.
[97] F.A. Morrison, Electrophoresis of a particle of arbitrary shape, J. Colloid Interface Sci. 34 (1970) 210–214. https://doi.org/10.1016/0021-9797(70)90171-2.
[98] O.D. Ernst, A. Vaghef-Koodehi, C. Dillis, A. Lomeli-Martin, B.H. Lapizco-Encinas, Dependence of Nonlinear Electrophoresis on Particle Size and Electrical Charge, Anal. Chem. 95 (2023) 6595–6602. https://doi.org/10.1021/acs.analchem.2c05595.
[99] O. Vesterberg, History of electrophoretic methods, J. Chromatogr. A. 480 (1989) 3–19. https://doi.org/10.1016/S0021-9673(01)84276-X.
[100] S. Hjertén, K. Elenbring, F. Kilár, J.-L. Liao, A.J.C. Chen, C.J. Siebert, M.-D. Zhu, Carrier-free zone electrophoresis, displacement electrophoresis and isoelectric focusing in a high-performance electrophoresis apparatus, J. Chromatogr. A. 403 (1987) 47–61. https://doi.org/https://doi.org/10.1016/S0021-9673(00)96340-4.
[101] R.C. Ebersole, R.M. McCormick, Separation and isolation of viable bacteria by capillary zone electrophoresis, Nat Biotech. 11 (1993) 1278–1282. https://doi.org/10.1038/nbt1193-1278.
[102] D.W. Armstrong, G. Schulte, J.M. Schneiderheinze, D.J. Westenberg, Separating Microbes in the Manner of Molecules. 1. Capillary Electrokinetic Approaches, Anal. Chem. 71 (1999) 5465–5469. https://doi.org/10.1021/ac990779z.
[103] M.J. Desai, D.W. Armstrong, Separation, identification, and characterization of microorganisms by capillary electrophoresis, Microbiol. Mol. Biol. Rev. 67 (2003) 38–51. https://doi.org/10.1128/mmbr.67.1.38-51.2003.
[104] M. Girod, D.W. Armstrong, Monitoring the migration behavior of living microorganisms in capillary electrophoresis using laser-induced fluorescence detection with a charge-coupled device imaging system, Electrophoresis. 23 (2002) 2048–2056. https://doi.org/10.1002/1522-2683(200207)23:13<2048::AID-ELPS2048>3.0.CO;2-T.
[105] E. Dziubakiewicz, B. Buszewski, Capillary electrophoresis of microbial aggregates, Electrophoresis. 35 (2014) 1160–1164. https://doi.org/10.1002/elps.201300588.
[106] B. Buszewski, E. Kłodzińska, Determination of pathogenic bacteria by CZE with surface-modified capillaries, Electrophoresis. 29 (2008) 4177–4184. https://doi.org/10.1002/elps.200800080.
[107] J.N. Mehrishi, J. Bauer, Electrophoresis of cells and the biological relevance of surface charge, Electrophoresis. 23 (2002) 1984–1994. https://doi.org/10.1002/1522-2683(200207)23:13<1984::AID-ELPS1984>3.0.CO;2-U.
[108] M. Szumski, E. Kłodzińska, B. Buszewski, Separation of microorganisms using electromigration

techniques, J. Chromatogr. A. 1084 (2005) 186–193. https://doi.org/https://doi.org/10.1016/j.chroma.2004.09.062.

[109] M. Horká, P. Karásek, F. Růžička, M. Dvořáčková, M. Sittová, M. Roth, Separation of Methicillin-Resistant from Methicillin-Susceptible Staphylococcus aureus by Electrophoretic Methods in Fused Silica Capillaries Etched with Supercritical Water, Anal. Chem. 86 (2014) 9701–9708. https://doi.org/10.1021/ac502254f.

[110] J. Šalplachta, M. Horká, F. Růžička, K. Šlais, Identification of bacterial uropathogens by preparative isoelectric focusing and matrix-assisted laser desorption/ionization time-of-flight mass spectrometry, J. Chromatogr. A. 1532 (2018) 232–237. https://doi.org/10.1016/j.chroma.2017.11.072.

[111] M. Horká, J. Šalplachta, P. Karásek, F. Růžička, D. Štveráková, R. Pantůček, M. Roth, Rapid Isolation, Propagation, and Online Analysis of a Small Number of Therapeutic Staphylococcal Bacteriophages from a Complex Matrix, ACS Infect. Dis. 6 (2020) 2745–2755. https://doi.org/10.1021/acsinfecdis.0c00358.

[112] D.W. Armstrong, J.M. Schneiderheinze, J.P. Kullman, L.F. He, Rapid CE microbial assays for consumer products that contain active bacteria, FEMS Microbiol. Lett. 194 (2001) 33–37. https://doi.org/10.1111/j.1574-6968.2001.tb09442.x.

[113] D.W. Armstrong, L. He, Determination of cell viability in single or mixed samples using capillary electrophoresis laser-induced fluorescence microfluidic systems, Anal. Chem. 73 (2001) 4551–4557. https://doi.org/10.1021/ac010449q.

[114] B.A. Jucker, H. Harms, A.J.B. Zehnder, Adhesion of the positively charged bacterium Stenotrophomonas (Xanthomonas) maltophilia 70401 to glass and teflon, J. Bacteriol. 178 (1996) 5472–5479. https://doi.org/10.1128/jb.178.18.5472-5479.1996.

[115] E. Kłodzińska, M. Szumski, E. Dziubakiewicz, K. Hrynkiewicz, E. Skwarek, W. Janusz, B. Buszewski, Effect of zeta potential value on bacterial behavior during electrophoretic separation, Electrophoresis. 31 (2010) 1590–1596. https://doi.org/10.1002/elps.200900559.

[116] M.G. Bonomo, C. Cafaro, A. Guerrieri, F. Crispo, L. Milella, L. Calabrone, G. Salzano, Flow cytometry and capillary electrophoresis analyses in ethanol-stressed oenococcus oeni strains and changes assessment of membrane fatty acid composition, J. Appl. Microbiol. 122 (2017) 1615–1626. https://doi.org/10.1111/jam.13466.

[117] W. Kupczyk, E. Maślak, V. Railean-Plugaru, P. Pomastowski, M. Jackowski, B. Buszewski, Capillary Zone Electrophoresis in Tandem with Flow Cytometry in Viability Study of Various ATCC Bacterial Strains under Antibiotic Treatment, Int. J. Environ. Res. Public Health. 19 (2022). https://doi.org/10.3390/ijerph19031833.

[118] E. Maślak, W. Kupczyk, V. Railean, P. Pomastowski, M. Jackowski, B. Buszewski, Viability study of

clinical bacterial strains by capillary electrophoresis and flow cytometry approaches, Electrophoresis. 43 (2022) 2005–2013. https://doi.org/10.1002/elps.202200096.

[119] V. Kasarabada, N.N. Nasir Ahamed, A. Vaghef-Koodehi, G. Martinez, B.H. Lapizco-Encinas, N. Nihaar, N. Ahamed, A. Vaghef-Koodehi, G. Martinez-Martinez, B.H. Lapizco-Encinas, Separating the Living from the Dead: An Electrophoretic Approach, Anal. Chem. 96 (2024) 15711–15719. https://doi.org/10.1021/acs.analchem.4c03336.

[120] B.H. Lapizco-Encinas, B.A. Simmons, E.B. Cummings, Y. Fintschenko, Dielectrophoretic Concentration and Separation of Live and Dead Bacteria in an Array of Insulators, Anal. Chem. 76 (2004) 1571–1579. https://doi.org/10.1021/ac034804j.

[121] F. Crispo, A. Capece, A. Guerrieri, P. Romano, Capillary zone electrophoresis as alternative tool for rapid identification and quantification of viable Saccharomyces cerevisiae cells, LWT - Food Sci. Technol. 68 (2016) 506–513. https://doi.org/10.1016/j.lwt.2015.12.026.

TABLES

Table 1. Summary of the reports on dielectrophoresis-based cell viability assessments and separations.

Bacterial cells			
Cell type	**Description of the system employed**	**Electric stimulation**	**Year and ref.**
S. aureus	Microdevice containing 3D embedded insulating micropillars.	AC voltages up to 400 Vpp at frequencies from 30 to 60 kHz. DC-biased AC voltages with 10 to 20 VDC and up to 200 Vpp at frequencies from 2 kHz and 400 kHz.	2015 [28,29]
S. epidermis	Monolithic device that combines off- chip passivated insulator-based dielectrophoresis and bioimpedance measurements for	AC voltages up to 300 Vpp at frequencies from 100 to 400 kHz.	2018 [30]
E. coli and *S. cerevisiae*	Combination of DEP and deterministic lateral displacement (DLD). Sorting device with a dense array of insulating pillars, and three distinct outlets that allowed for collection of separated cell fractions.	AC voltages up to 600 Vpp at frequencies from 1 Hz to 20 kHz.	2021 [8]
C. difficile	Microchannels with sharp lateral constrictions that reduce channel width from 1000 μm to only 15 μm.	AC voltages up to 300 Vpp at frequencies from 50 kHz to 1 MHz.	2018 [35]
E. coli and *S. Typhi*	Microdevice with microwells that contained circular photoconductive electrodes	AC voltages in the range of 5 to 20 Vpp at frequencies from 50 kHz to 20 MHz.	2018 [36]
S. Typhi , *E. faecalis* and *S. aureus*	Microdevice that combined DEP and impedance spectroscopy that featured reusable interdigitated electrodes.	AC voltages of 20 Vpp at a frequency of 5 MHz.	2021 [37]
E. coli and *E. faecalis*	Microfluidic chambers filled with silica microbeads used to inactivate bacteria.	DC voltages up to 400 V to generate electric fields up to 2 kV/cm.	2020 [39]
E. coli and *E. faecalis*	Microchannels with an array of insulating micropillars are used to electroporate cells and induce cell death.	DC voltages to generate electric fields up to 167 V/cm. AC voltages up to 300 V and frequencies from 2.5 kHz to 100 kHz.	2021 [40]
Yeast cells			

Cell type	Description of the system employed	Electric stimulation	Year and ref.
S. cerevisiae	Rudimentary, the system had a cup-shaped cavity that contained a pin and plate electrodes.	AC voltages up to 200 V (rms) @ 2.55 MHz.	1966, 1968 [24,25]
S. cerevisiae	Combination of DEP and deterministic lateral displacement (DLD). Sorting device with a dense array of insulating pillars, and three distinct outlets that allowed for collection of separated cell fractions.	AC voltages up to 600 Vpp at frequencies from 1 Hz to 20 kHz.	2021 [8]
S. cerevisiae	Microchannels with an array of insulating micropillars are used to electroporate cells and induce cell death.	DC voltages up to 900 V [38].	2019 [38]
S. cerevisiae and red cabbage protoplast cells	Microfluidic chamber with top and bottom thin electrodes, live cells were attracted to the electrodes.	AC voltages up to 1.5 Vpp at frequencies from 300 kHz to 15 MHz.	2015 [41]
S. cerevisiae	Microdevice with bipolar electrodes where cell death was induced by increasing the temperature from 30 to 70 ^{o}C.	AC voltages up to 4 Vpp at frequencies from 10 kHz to 15 MHz.	2017 [42]
S. cerevisiae	Microdevice with two electrodes positioned forming a funnel configuration.	AC voltages up to 15 Vpp at frequencies from 0.03 MHz to 1 MHz.	2019 [43]
S. cerevisiae	Integrated CMOS DEP-based device with interdigitated electrode arrays.	AC voltages up to 20 Vpp at frequencies from 1 kHz to 20 MHz.	2020, 2021 [44,45]
S. cerevisiae	Integrated multiplexed system that combined acoustic and electric fields. DEP and DLD was induced with bipolar electrodes.	AC voltages up to 10 Vpp at frequencies from 50 Hz to 10 MHz.	2021 [46]
S. cerevisiae	System with micro-parallel cylindrical electrodes.	AC voltages from 1.5 to 14 Vpp at frequencies from 50 kHz to 4 MHz.	2023 [47]
Mammalian cells			
Cell type	**Description of the system employed**	**Electric stimulation**	**Year and ref.**
Chinese hamster ovary	Microdevice with a microfluidic channel with DEP actuation electrodes operated at dual frequencies, this system was referred as a DEP cytometer.	AC voltages up to 3 Vpp employing Frequency 1 = 300 kHz and frequency 2 = 6 to 7 MHz.	2016, 2019 [6,48]
Chinese hamster ovary	Microfluidic device with an array of embedded electrodes at the channel bottom.	AC voltages up to 3 Vpp at frequencies from 50 Hz to 10 MHz.	2018 [49]
Chinese hamster ovary	Microdevice with actuation electrodes that measures the dielectric spectrum of single cells while they flow through a microfluidic channel.	AC voltages up to 3 Vpp at frequencies from 10 kHz to 3 MHz.	2019 [50]
Neural stem and progenitor cells	Device with a large capacity electrode array that enabled the selective enrichment of viable cells.	AC voltages up to 7 Vpp at frequencies from 80 kHz to 1 MHz.	2018 [51]
Rat adipose stem cells	Microsystem with 3-dimensional carbon electrodes equipped with a robotic that "picked and transferred" target cells.	AC voltages up to 20 Vpp at frequencies from 10 kHz to 5 MHz.	2019 [52]
Dental pulp stromal cells	Microsystem with two sets of opposing interdigitated transducers that combined surface acoustic waves (SAW) and DEP effects.	SAW induced electric field at a frequency of 10 MHz.	2017 [53]
U937 monocytes	Microsystem with 3-dimensional carbon electrodes.	AC voltages up to 20 Vpp at frequencies from 50 kHz to 1 MHz.	2017 [55]
Jurkat cells as proxies for T-lymphocytes	Device with micro-fabricated interdigitated electrode array (IDE).	DC voltages of 12 V for electroporation. AC voltages up to 6 Vpp at frequencies from 100 Hz to 5 MHz.	2019 [56]
T-lymphocytes	Microfluidic device with castellated electrodes, a single inlet and two outlets.	AC voltages up to 5 Vpp at frequencies from 150 Hz to 150 MHz.	2022 [57]
Cancer cells			
Cell type	**Description of the system employed**	**Electric stimulation**	**Year and ref.**

Human prostate cancer (PC-3)	Microdevice with 3-dimeniosnal self-assembled ionic liquid electrodes that featured a conductivity gradient to induce pDEP on target cells.	AC voltages up to 400 Vpp at frequencies from 10 kHz to 10 MHz.	2016 [60]
HeLA	Commercially available system 3DEP (DEPtech). The system is a well-based DEO cytometer that employs 20 parallel 3-dimensinal electrode arrays.	AC voltages up to 400 Vpp at frequencies from 10 kHz to 20 MHz.	2016 [59]
Non-small cell lung cancer	Microdevice with an array of interdigitated electrode system.	AC voltages up to 10 Vpp at frequencies from 1 kHz to 100 MHz.	2016 [66]
Pancreatic ductal adenocarcinoma	Microdevice where DEP effects were optically generated employing a beam of light that served as a virtual electrode array.	NA – this system was optically stimulated.	2019 [67]
Chemo-resistant circulating pancreatic cancer cells	Microdevice with a DLD array that featured three distinct outlets, one outlet for each of the three DEP response types.	AC voltages from 15 to 45 Vpp at frequencies from 0.1 to 1 MHz.	2024 [68]
Pancreatic cancer	Device for electrorotation with hyperbolic 4-electrode geometry. Data obtained with electrorotation was used to predict DEP spectra.	AC voltages from 15 to 45 Vpp at frequencies from 100 Hz to 100 MHz.	2016 [69]
Human leukemia (K562)	Device that integrated hydrodynamic focusing and DEP. The device featured a narrow constriction located prior interdigitated electrode array.	AC voltages of 3.8 Vpp at frequencies of 1 MHz.	2023 [70]

Table 2. Summary of the reports on electrophoresis-based cell viability assessments and separations.

Bacterial cells			
Cell type	**Description of the system employed**	**Electric stimulation**	**Year and ref.**
L. acidophilus,	CE system with a 100 µm diameter fused silica capillary, 27 cm long with, with the interrogation window located at 20 cm from the capillary inlet. UV detection was employed.	DC voltages, separation performed at 10 kV.	2001 [112]
B. infantis and cerevisiae	CE system with a 100 µm diameter fused silica capillary, 30 cm long with, with the interrogation window located at 20 cm from the capillary inlet. LIF detection was employed.	DC voltages, separation performed at 15 kV.	2001 [113]
O. oeni	CE system with a 100 µm diameter fused silica capillary, 49.5 cm long with, with the interrogation window located at 38.5 cm from the capillary inlet. Diode array detection was employed.	DC voltages, separation performed at 10 kV.	2017 [116]
E. faecalis, *S. aureus, K. pneumoniae, P. aeruginosa and E. coli.*	CE system with a 75 µm diameter quartz capillary, 33.5 cm long with, with the interrogation window located at 25 cm from the capillary inlet. Diode array detection was employed.	DC voltages, separation performed at 15 kV.	2022 [117]
MRSA, MSSA and *E. coli*	CE system with a 75 µm diameter fused silica capillary, 33.5 cm long with, with the interrogation window located at 25 cm from the capillary inlet. Diode array detection was employed.	DC voltages, separation performed at 15 kV.	2022 [118]
E. coli	Insulator-based electrokinetic (iEK) microchannel with a T-cross configuration for EK injection. Channel was 51.53 mm long, 1.1 mm wide and had an array of cylindrical insulating pillars.	DC voltages, separation performed at an overall electric field of 137.4 V/cm.	2024 [119]
E. coli	Insulator-based electrokinetic (iEK) microchannel with a T-cross configuration for EK injection. Channel was 10.2 mm long, 1.0 mm wide and had an array of cylindrical insulating pillars.	DC voltages, separation performed at an overall electric field of 600 V/cm	2004 [120]
Yeast cells			
Cell type	**Description of the system employed**	**Electric stimulation**	**Year and ref.**

S. cerevisiae	CE system with a 100 µm diameter bare fused silica capillary, with the interrogation window located at 21 cm from the capillary inlet. Diode array detection was employed.	DC voltages, separation performed at 10 kV.	2016 [121]

1103